

# Cellular Automata in ecohydraulics modeling: principles, scales and applications

Qiuwen Chen

Nanjing Hydraulic Research Institute, China

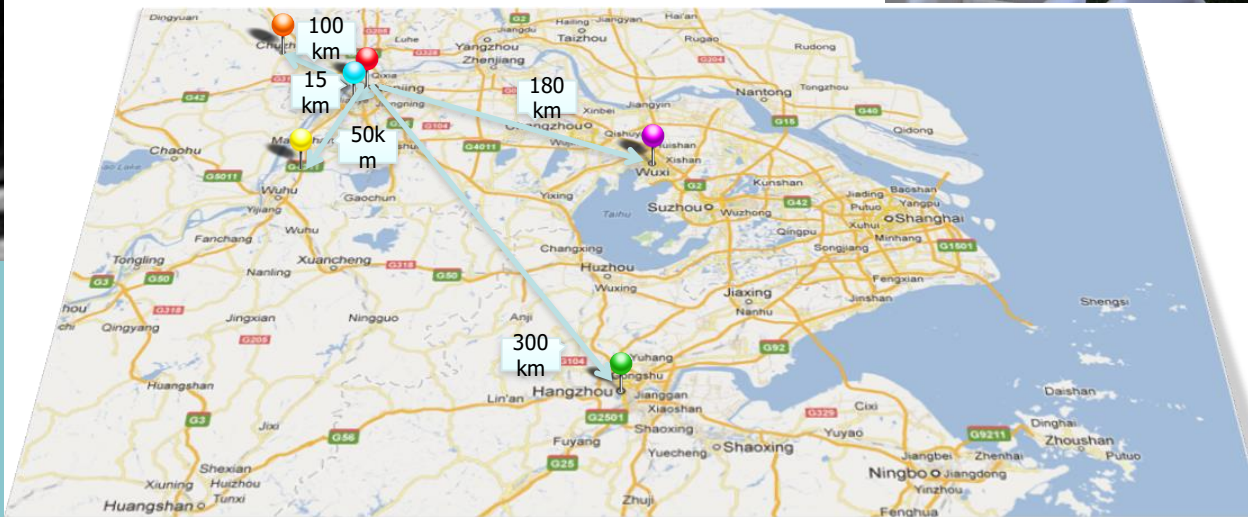
1935



### PhD Program

- River Hydraulics
- Port, coast and offshore.
- Water resources
- Hydro-power engineering
- Hydraulic structures

NHRI



China  
National  
Hydraulic  
Research  
Institute



2009



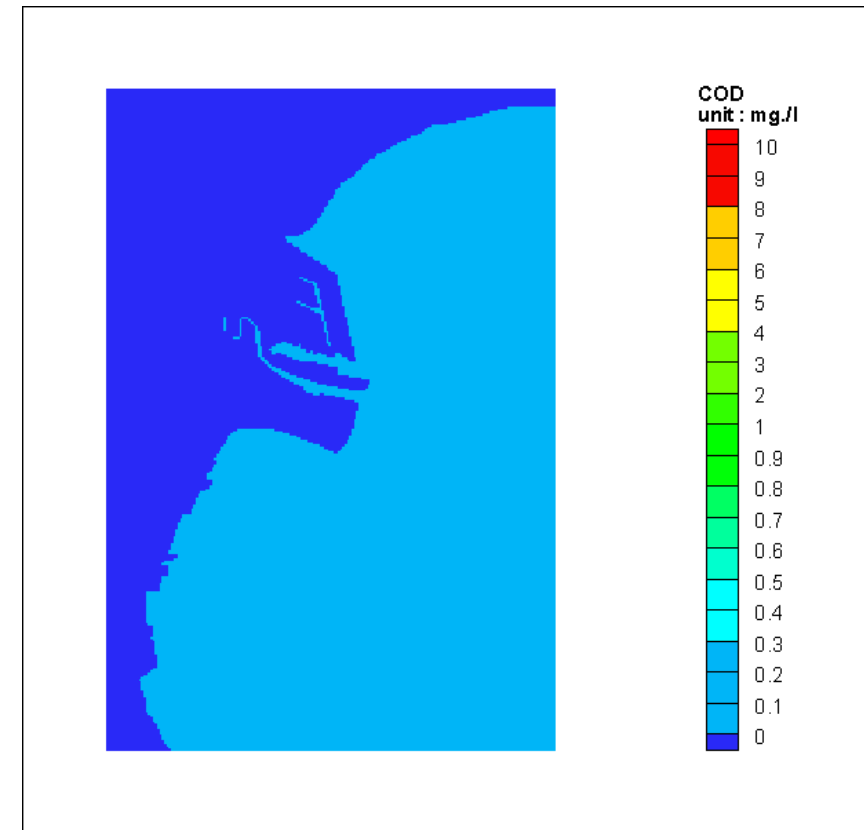
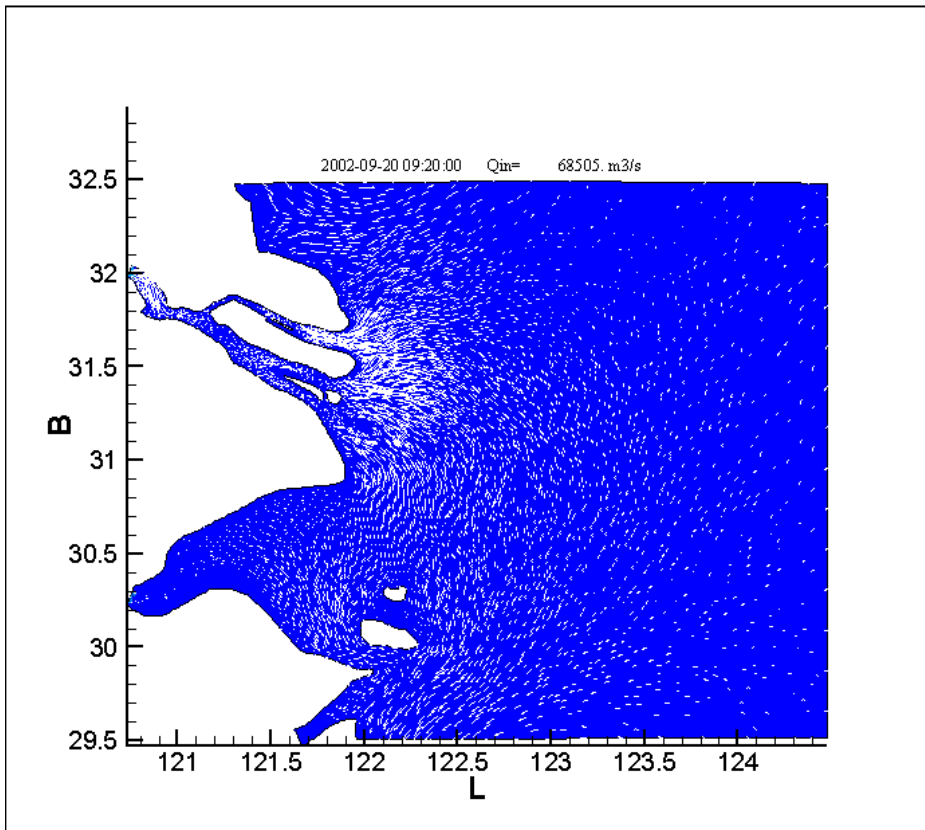
Nanjing  
Hydraulic  
Research  
Institute, MWR,  
MOT, NEA

# 1. Principles in continuous world

## □ Continuity and homogeneity in hydrodynamics

$$\frac{\partial \vec{V}}{\partial t} + (\vec{V} \bullet \nabla) \vec{V} = \vec{F} - \frac{1}{\rho} \nabla P + \nu \nabla^2 \vec{V} \quad \nabla \bullet \vec{V} = 0$$

$$\frac{\partial c}{\partial t} + u \frac{\partial c}{\partial x} + v \frac{\partial c}{\partial y} + w \frac{\partial c}{\partial z} = D_x \frac{\partial^2 c}{\partial x^2} + D_y \frac{\partial^2 c}{\partial y^2} + D_z \frac{\partial^2 c}{\partial z^2} + S + f_R(c, t)$$



# 1. Principles in discontinuous world

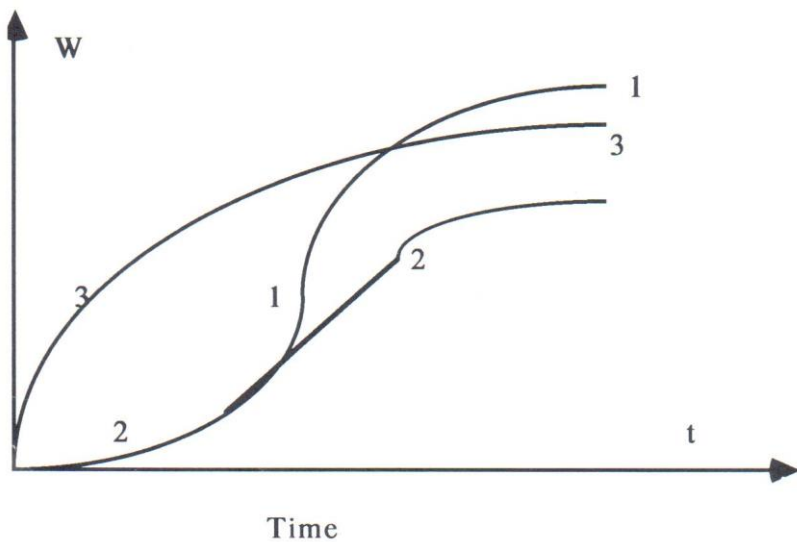
## □ Peso-continuity and homogeneity in eco-dynamics

$$r(t) = r_{\max} \frac{C}{K_s + C}$$

Michaelis-Menten

$$\frac{dN}{dt} = rN(1 - \frac{N}{K})$$

Logistic growth



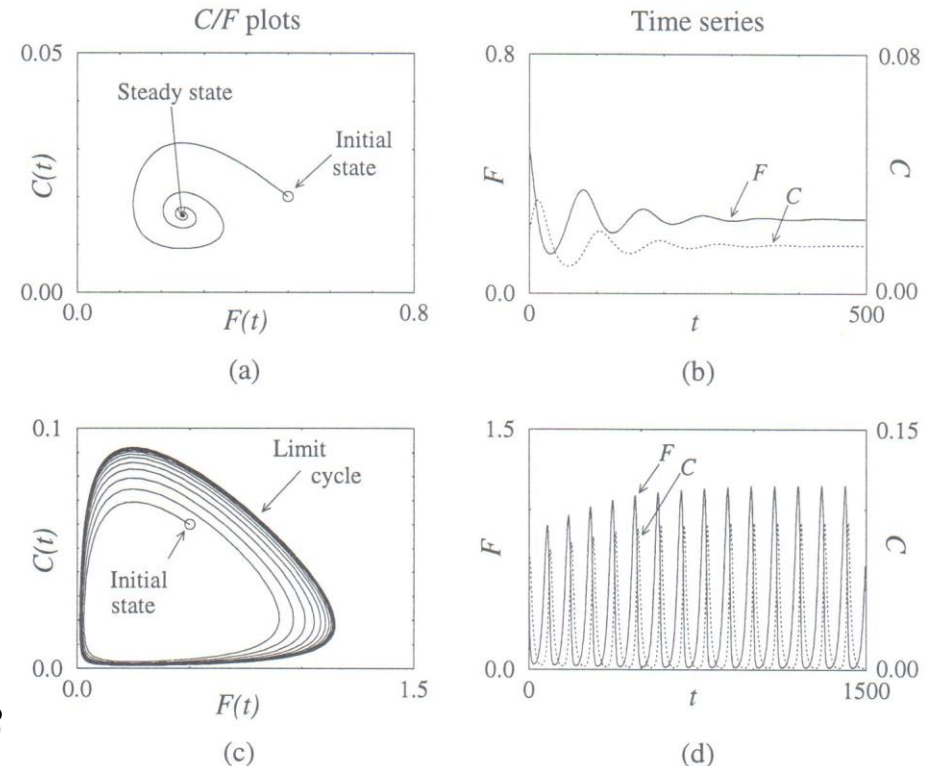
S.E. Jorgensen, Fund. of Ecol. Mod., 1994

W.S. Gurney & R. Nisbet, Ecol. Dyna., 1998

$$\frac{dN}{dt} = rN - \alpha NP$$

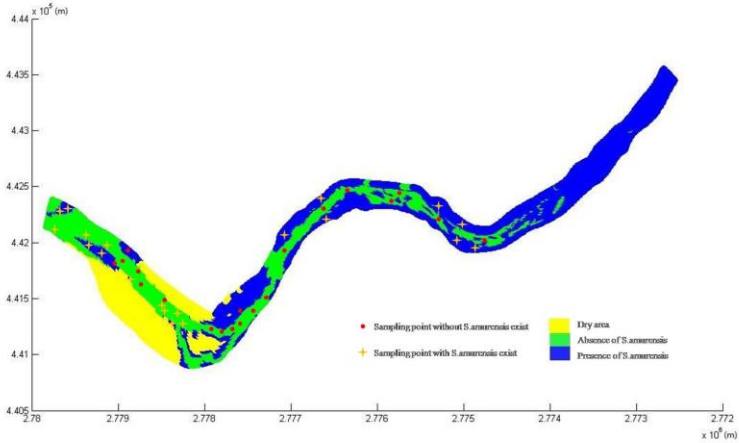
Lotka-Volterra

$$\frac{dP}{dt} = -cP + \beta NP$$

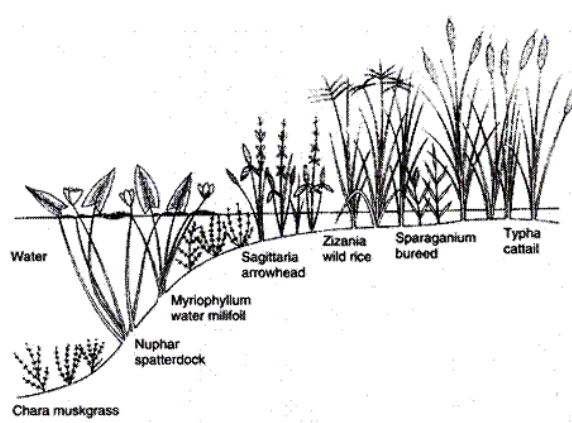


# 1. Principles in discontinuous world

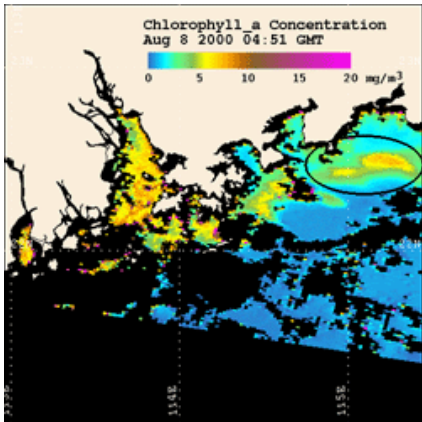
## ❑ Facts of aquatic eco-dynamics: discontinuity & heterogeneity



Discrete state: presence/absence



Local vs. global interactions



Spatial heterogeneity

Discontinuous reproduction

Discontinuous predation

# 1. Principles in discontinuous world

## □ Challenges in linking fluid dynamics & eco-dynamics

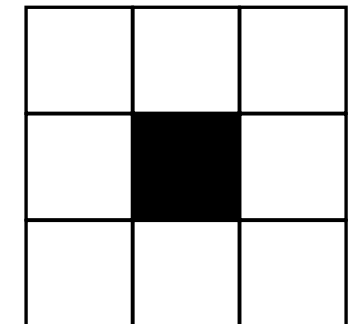
- ✧ Discrete state
- ✧ Individual difference
- ✧ Local interactions



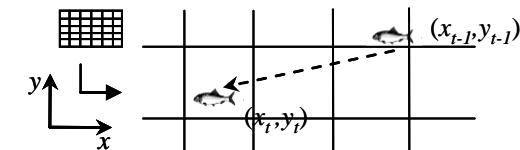
## □ Innovative solution to eco-hydraulics modelling

Cellular automata: discrete in time and space, reproduce complex spatial-temporal dynamic patterns by some simple local interaction rules between cells.

$$a_{i,j}^{t+1} = f(a_{i-1,j-1}^t, a_{i-1,j}^t, a_{i-1,j+1}^t, a_{i,j-1}^t, a_{i,j}^t, a_{i,j+1}^t, a_{i+1,j-1}^t, a_{i+1,j}^t, a_{i+1,j+1}^t)$$



Individual based: describe individual properties & behaviours, interactions between individuals, individual & environments.



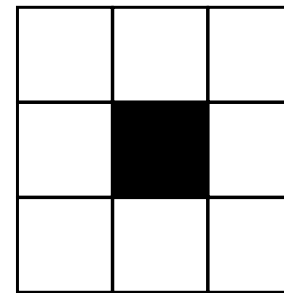
# 1. Principles in discontinuous world

## □ Cellular Automata

- ① A mathematical system, discrete in space and time
- ② Consist of a regular lattice of cells (automaton)
- ③ Each cell has finite possible states
- ④ Cell state updates according to local interactions
- ⑤ Global complex patterns emerge through evolutions



$$a_i^{t+1} = f(a_{i-1}^t, a_i^t, a_{i+1}^t)$$



$$a_{i,j}^{t+1} = f(a_{i-1,j-1}^t, a_{i-1,j}^t, a_{i-1,j+1}^t, a_{i,j-1}^t, a_{i,j}^t, a_{i,j+1}^t, a_{i+1,j-1}^t, a_{i+1,j}^t, a_{i+1,j+1}^t)$$

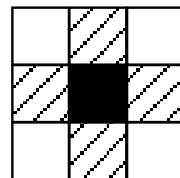
❖ Local behaviours   ❖ Spatially explicit   ❖ Patchy phenomena

# 1. Principles in discontinuous world

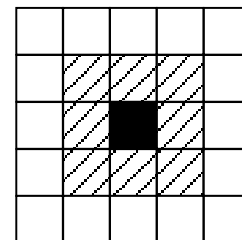
## □ Cellular Automata: neighbor scheme



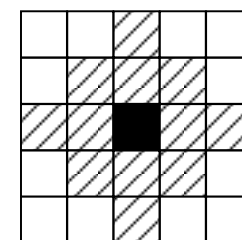
1D Moore



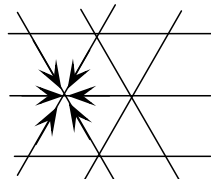
Von Neumann



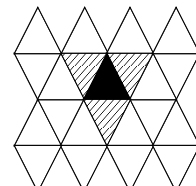
2D Moore



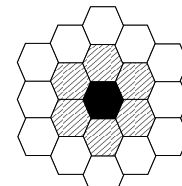
Extended Moore



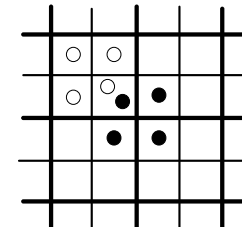
Lattice gas



Triangular



Hexagon



Margolus

# 1. Principles in discontinuous world

## □ Cellular Automata: initial condition

- ✧ In close automata, initial condition is not sensitive due to memoryless
- ✧ In open automata, external governing factor are incorporated, initial condition must be correctly set

## □ Cellular Automata: boundary conditions

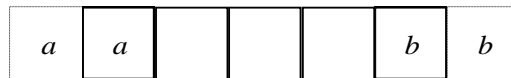
- ✧ In modelling practice, CA must be finite and have boundaries



Period boundary



Fixed boundary



Adiabatic boundary



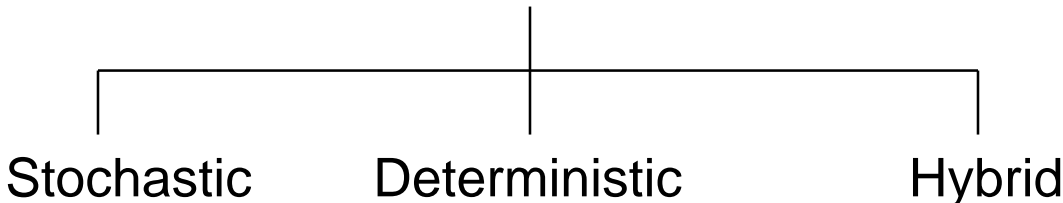
Reflection boundary

# 1. Principles in discontinuous world

## □ Cellular Automata: evolution rules

$$a_{i,j}^{t+1} = f(a_{i-1,j-1}^t, a_{i-1,j}^t, a_{i-1,j+1}^t, a_{i,j-1}^t, a_{i,j}^t, a_{i,j+1}^t, a_{i+1,j-1}^t, a_{i+1,j}^t, a_{i+1,j+1}^t)$$

- ④  $f$ : evolution rules define cell updating



- ④ Usually totalistic or outer totalistic rule are used

$$C = \sum_n f(n) k^n$$

$$\tilde{C} = \sum_n \tilde{f}[a,n] k^{kn+a}$$

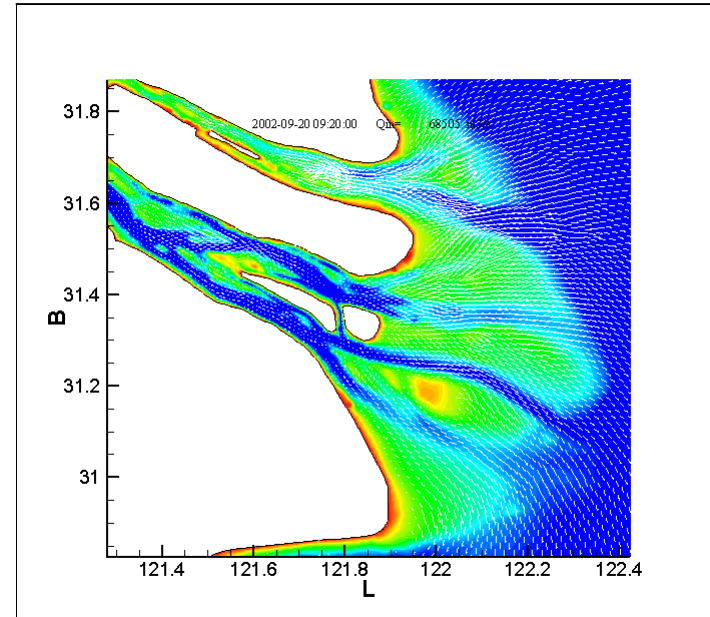
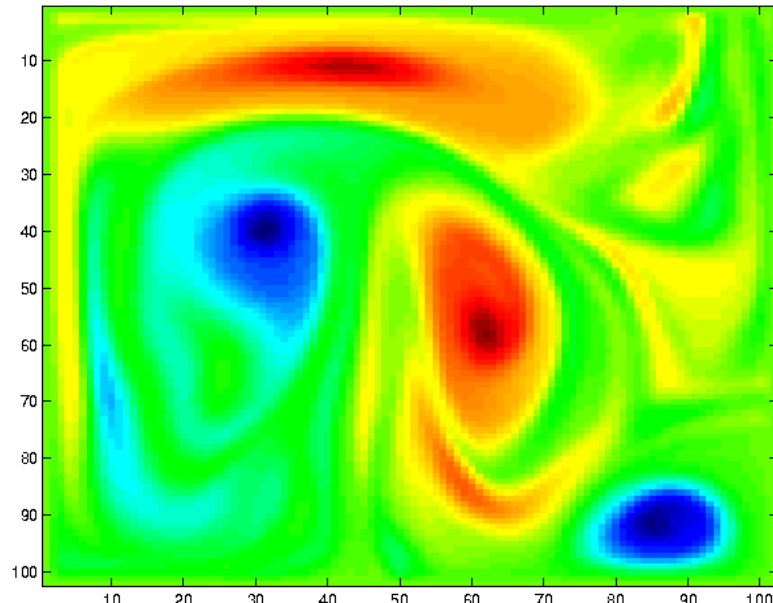


(Von Neumann, 1949)

# 2. Scales in eco-hydraulic model

## □ Scales in hydrodynamic model

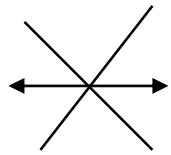
- ✧ Direct numerical simulation (DNS):  $\Delta x = \Delta t/2$ ,  $\Delta$  Kolmogorov length scale
- ✧ Large eddy simulation (LES):  $\Delta x > \Delta t/2$
- ✧ Reynolds averaged N-S simulation (RANS): engineering scale  $C_r = \frac{u\Delta t}{\Delta x}$



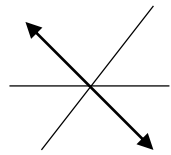
(from *Firmijn Zijl, 2002, TUD*)

## 2. Scales in eco-hydraulic model

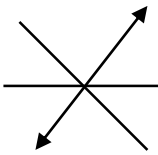
### □ Scales in lattice gas model



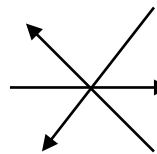
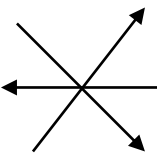
(two particles)



or



(three particles)



$$n_i(x + \lambda c_i, t + \tau) = n_i(x, t) + \Delta_i[n(x, t)]$$

$$c_i = (\cos \pi i / 3, \sin \pi i / 3) \quad u_i = \lambda c_i / \tau \quad \rho(x, t) = \sum_{i=1}^6 N_i(x, t)$$

$$\sum_i n_i(x + \lambda c_i, t + \tau) = \sum_i n_i(x, t)$$



(Wolfram, 1984)

$$\sum_i u_i n_i(x + \lambda c_i, t + \tau) = \sum_i u_i n_i(x, t)$$

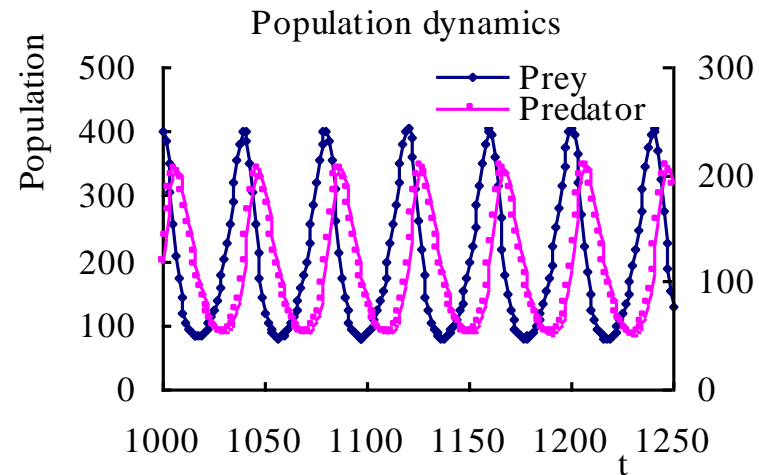
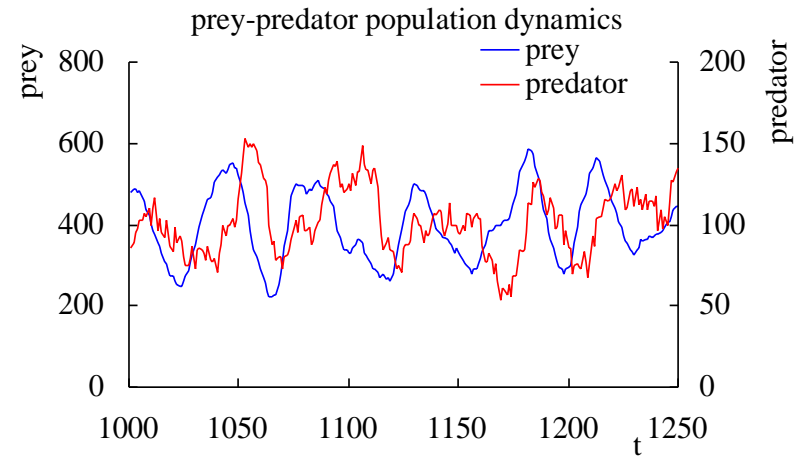
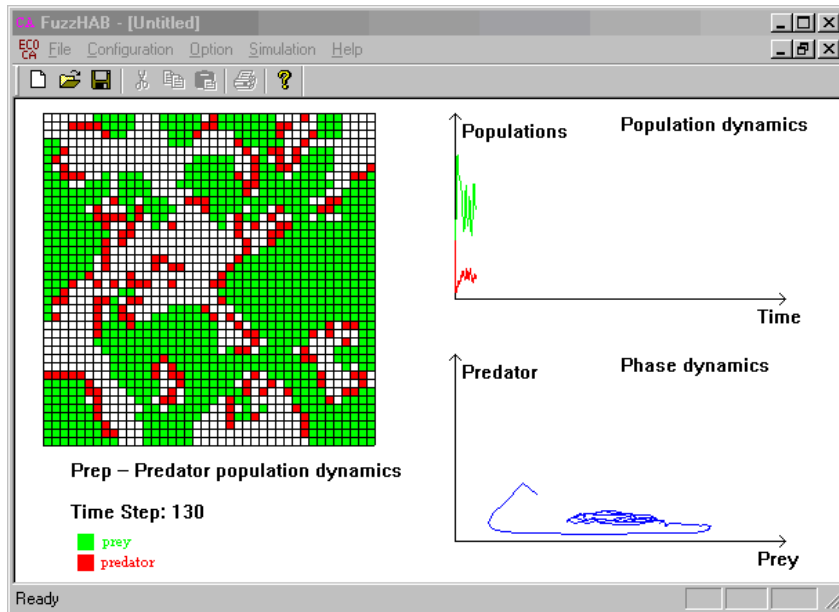
$$\partial_t(u) + (u \nabla)u = -\frac{1}{\rho g(\rho)} \nabla p + \nu \nabla^2 u \quad \nu = \frac{1}{g(\rho)} \left( \frac{1}{2\rho(1-\frac{\rho}{6})^3} - \frac{1}{8} \right)$$

✧ unit  $\text{at}$ , unit  $\text{ax}$ , Boolean state, high gradient



# 2. Scales in eco-hydraulic model

## Scales in two species dynamic model



- ⌚  $\bar{t}$ : mean predation time interval
- \_RADIUS\_  $\bar{x}$ : maximum searching radius

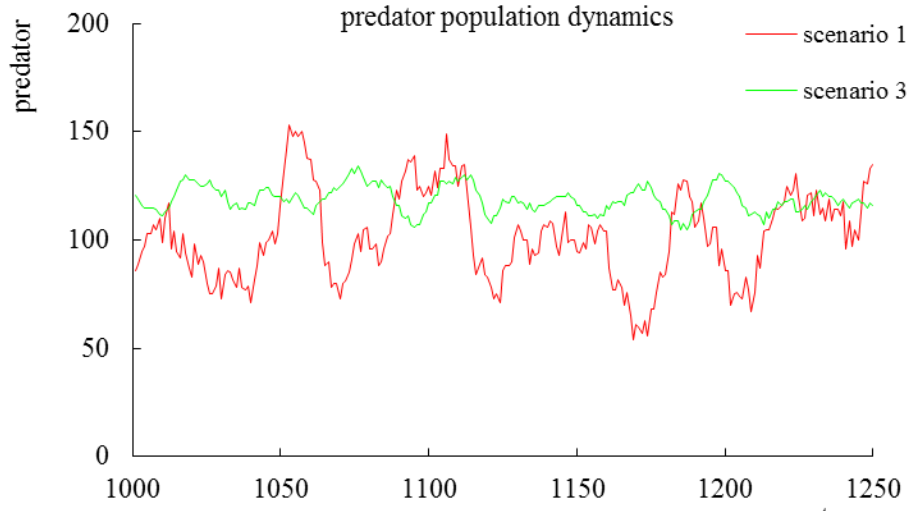
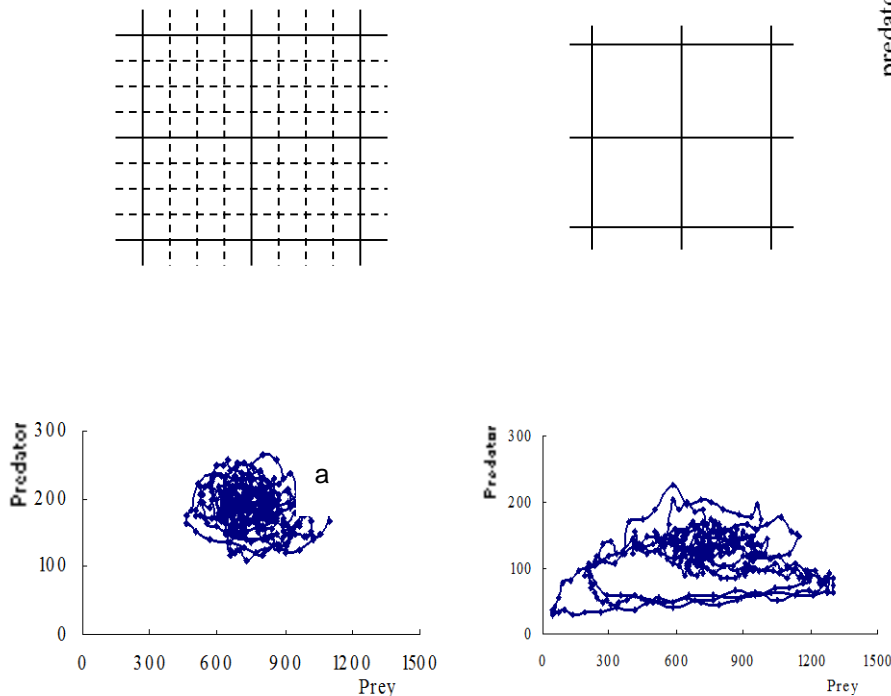
Qu et al, 2008, *Eco Inf*, 3: 252-258 (citations: 58)

Chen and Mynett., 2003, *SIMPRA*, 11: 609-625

$$\frac{dN}{dt} = rN - \alpha NP \quad \frac{dP}{dt} = -cP + \beta NP \quad \text{No } \bar{x}!!$$

## 2. Scales in eco-hydraulic model

### □ Scales in two species dynamic model

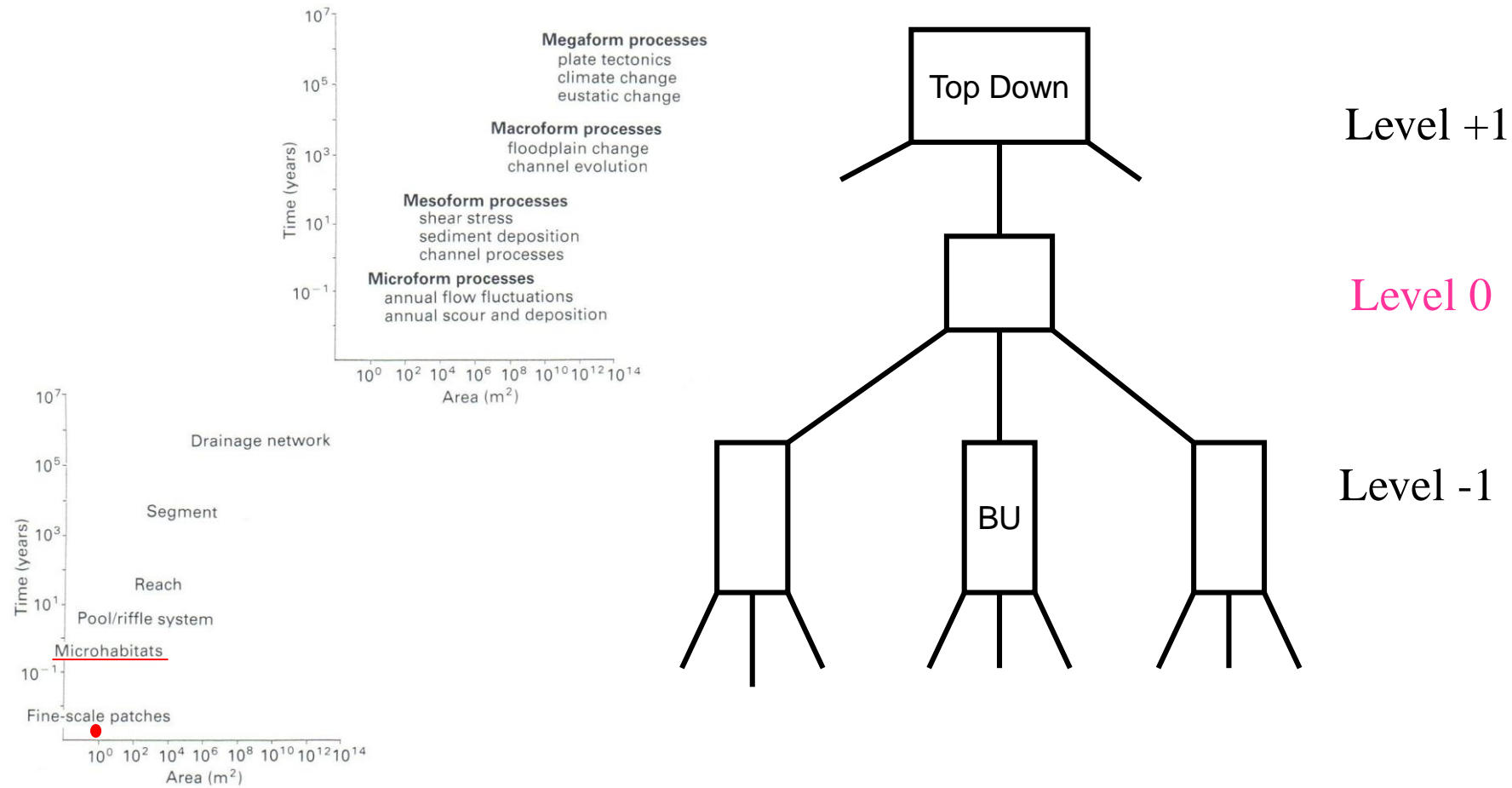


	Scenario 1		Scenario 2	
	Mean	Stdv.	Mean	Stdv.
Prey	397	89	382	24
Predator	106	23	118	6

- ✧ CA reveals the embedded structure stability
- ✧ Improper spatial scale ( ) creates artefact patterns

# 2. Scales in eco-hydraulic model

## □ Hierarchic scales in aquatic ecosystem



## 2. Scales in eco-hydraulic model

### □ Scales identification and coupling

#### ⓐ Spatial scale analysis (Gussian field)

$$\rho_{x, x+\Delta x} = \rho_0 + (1 - \rho_0) e^{-(\Delta x/L)^2}$$

$\rho_{x, x+\Delta x}$ : correlation between two spatial cells

$L$ : characteristic scale of studied system level

#### ⓑ Spatial scale analysis (Wavelet analysis)

$$\omega(\eta, x) = \frac{1}{a} \int_{-\infty}^{+\infty} f(x) g(x - \frac{\xi}{\eta}) dx \quad \omega(\eta) = \int_{-\infty}^{+\infty} \omega^2(\eta, x) dx$$

$\eta$  : scale factor;

$\xi$ : the point around which the Wavelet is centred.

❖ Cell size  $\Delta x \leq L/2$ ,  $\Delta t$  is determined according to  $\Delta x$ .

## 2. Scales in eco-hydraulic model

### □ Scales identification and coupling

- Ⓐ High frequency components: Upscaling

Simple averaging:

$$\overline{A(t)} = \frac{1}{N} \sum_{i=1}^N A_i$$

Weighted averaging:

$$\overline{A(t)} = \int_{\varepsilon} A(E') p(t, E') dE'$$

Power averaging:

$$\overline{A(t)} = \left[ \frac{1}{N} \sum_{i=1}^N A_i^p \right]^{\frac{1}{p}}$$

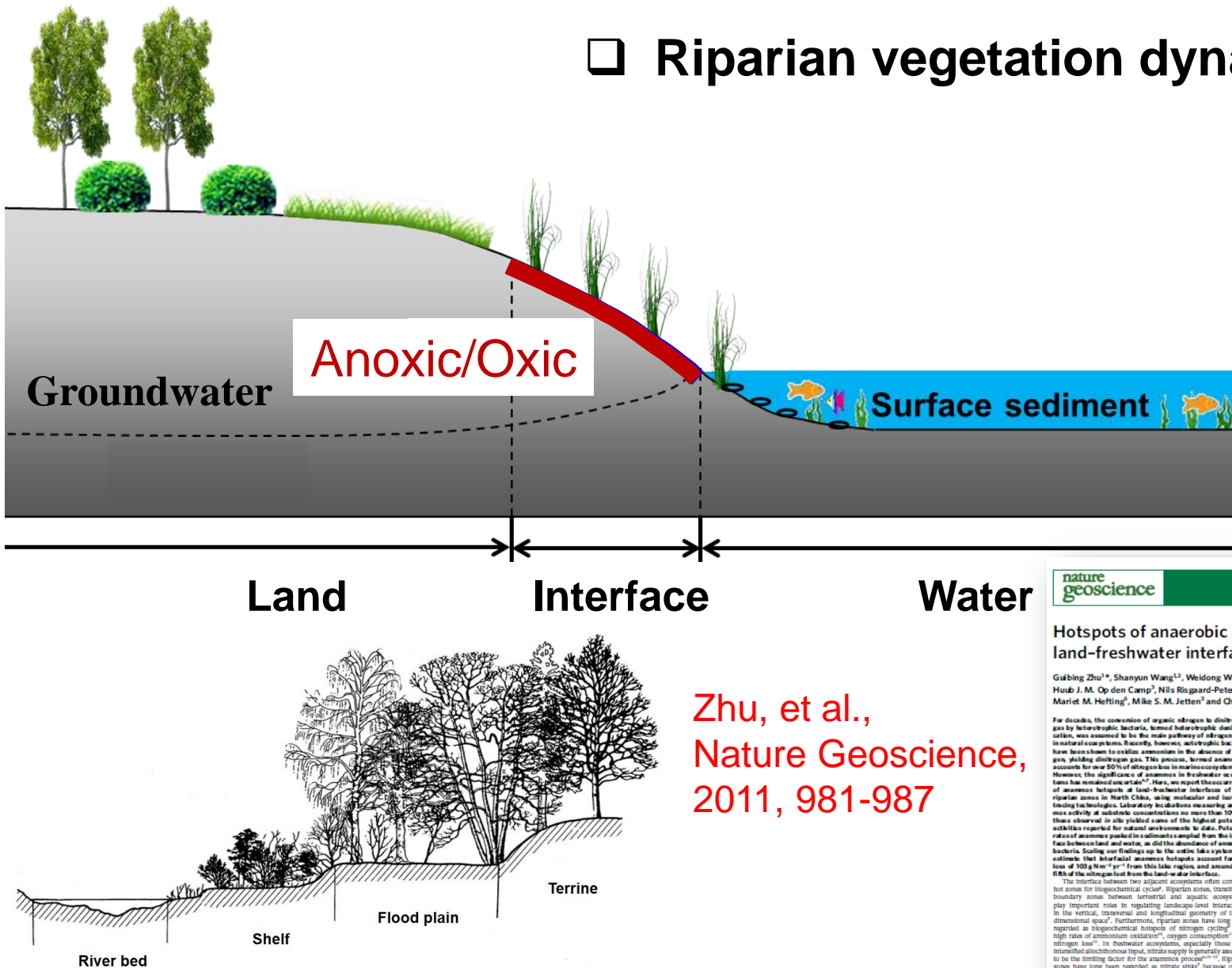
- Ⓑ Low frequency components: Downscaling

Use up level components as constraint to the dynamics of the studied level

$$a_{i,j}^{t+1} = f(Neb, For | B)$$

# 3. Applications in ecohydraulics

## □ Riparian vegetation dynamics



Zhu, et al.,  
Nature Geoscience,  
2011, 981-987

nature  
geoscience

PUBLISHED ONLINE: 6 JANUARY 2013 | DOI:10.1038/ngeo1663

### Hotspots of anaerobic ammonium oxidation at land-freshwater interfaces

Gubing Zhu<sup>1\*</sup>, Shanyun Wang<sup>1,2</sup>, Weidong Wang<sup>1</sup>, Yu Wang<sup>1</sup>, Leilu Zhou<sup>1</sup>, Bo Jiang<sup>1</sup>, Hubo J. M. Op den Camp<sup>3</sup>, Nils Risgaard-Petersen<sup>4</sup>, Lorenz Schwark<sup>5</sup>, Yongchen Peng<sup>2</sup>, Mariet M. Helming<sup>6</sup>, Mike S. M. Jetten<sup>1</sup> and Chengqing Yin<sup>1</sup>

For decades, the conversion of organic nitrogen to dinitrogen gas by heterotrophic bacteria, termed nitrification, was believed to be the sole mechanism of nitrogen mineralization in natural ecosystems. Recently, however, autotrophic bacteria have been shown to oxidize ammonium in the absence of oxygen, yielding dinitrogen gas. This process, termed ammonium oxidation, accounts for ~50% of the total nitrogen mineralization in lakes. However, the significance of ammonium in freshwater ecosystems has remained unclear<sup>1–3</sup>. Here, we report the occurrence of ammonium oxidation at the land–water interface of three riparian zones in North China, using molecular and isotopic tracing technologies. Laboratory incubations measuring ammonium oxidation rates showed that the ammonium oxidation rates observed in the soil yielded some of the highest potential activities reported for natural environments to date. Potential rates of ammonium oxidation were found to be highest at the interface between land and water, as did the abundance of ammonia bacteria. Scaling our findings up to the entire lake system, we estimate that ammonium oxidation contributes to the annual nitrogen loss of 102 g N m<sup>-2</sup> yr<sup>-1</sup> from this lake region, and around one fifth of the nitrogen lost from the land–water interface.

This study demonstrates that the riparian zone contains hot zones for biogeochemical cycles. Riparian zones, transitional wetland zones between terrestrial and aquatic ecosystems, play important roles in regulating landscape-level interactions in the environment, such as the exchange of matter and energy (three-dimensional space). Furthermore, riparian zones have long been regarded as biogeochemical hotspots of nitrogen cycling with high nitrogen input and output, especially those with high nitrogen loss<sup>4</sup>. In freshwater ecosystems, especially those with strong anthropogenic influence, ammonium supply is generally assumed to be the limiting factor for primary production. Riparian zones have long been regarded as nitrate sinks<sup>5</sup> because of the high nitrogen input and low nitrogen output. However, riparian zones have long been regarded as nitrate sinks<sup>5</sup> because of the high nitrogen input and low nitrogen output.

North China with well-developed riparian zones, was selected as the study site (Supplementary Fig. S1). The hypothesis that riparian zones are hotspots of ammonium bacteria needed to be confirmed first. The 16S rRNA genes of Planctomycetes and ammonia bacteria in the surface (0–5 cm) and ten subsurface (30–40 cm) soil layers were extracted from the riparian zones and the adjacent waterward soil (site E) harboring ammonium 16S rRNA genes which were used to detect the presence of ammonium bacteria (Supplementary Fig. S2 and Table S1).

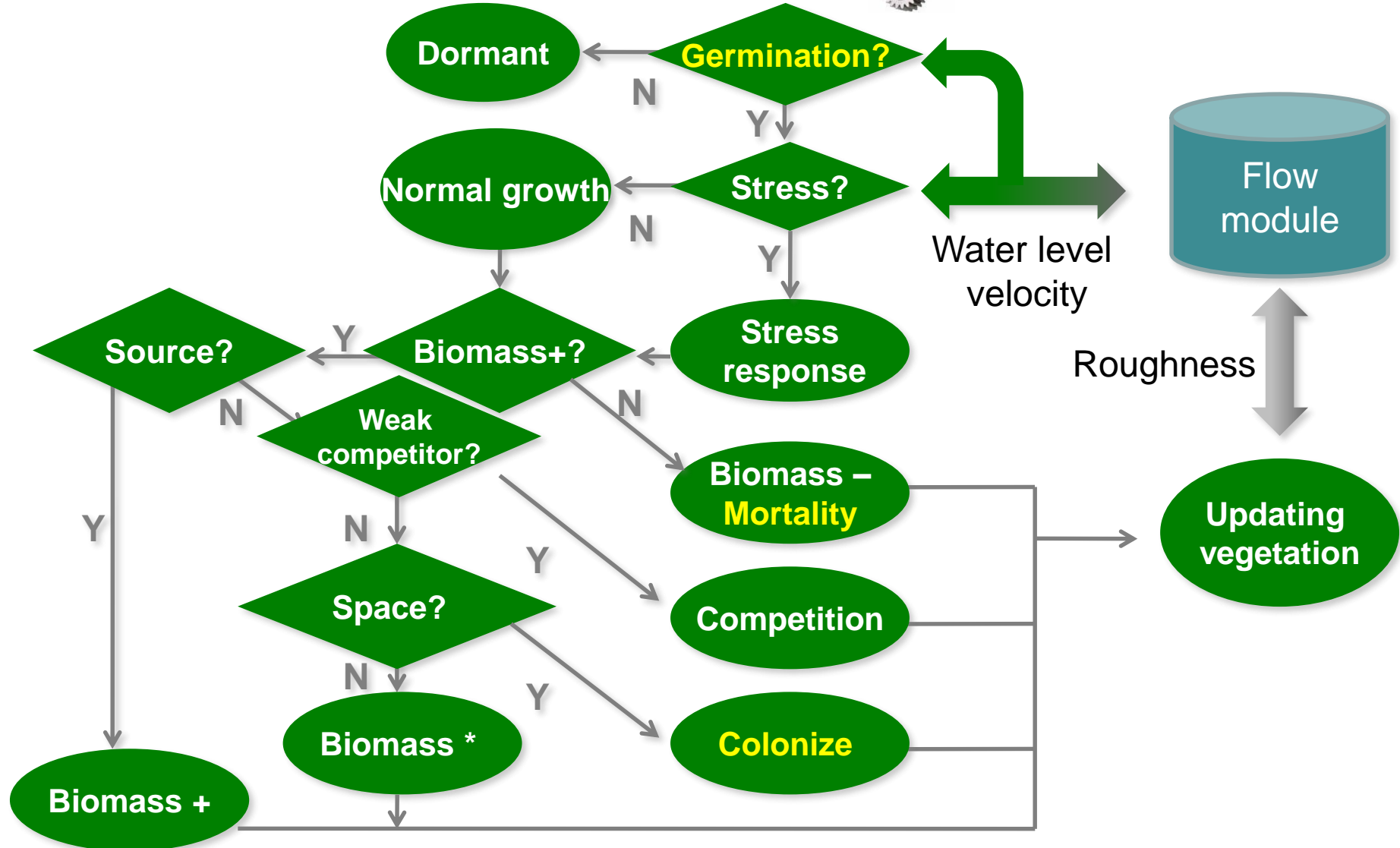
To investigate the distribution of ammonium bacteria in riparian zones, the presence of ammonium bacteria needed to be confirmed first. The 16S rRNA genes of Planctomycetes and ammonia bacteria in the surface (0–5 cm) and ten subsurface (30–40 cm) soil layers were extracted from the riparian zones and the adjacent waterward soil (site E) harboring ammonium 16S rRNA genes which were used to detect the presence of ammonium bacteria (Supplementary Fig. S2 and Table S1).

To address the occurrence of ammonium in particular hotspots, ammonium oxidation rates were measured in the riparian zones estimated using qPCR assays. The highest amount of hydrazine synthase (hzoB) gene was detected in interface sediments ( $1 \times 10^{10}$  copies/g dry weight) compared to the landward sediments ( $1 \times 10^9$  copies/g dry weight) and the adjacent waterward sediments ( $1 \times 10^9$  copies/g dry weight), whereas in the landward phase (site D and E) the hzoB gene was not detected (Supplementary Fig. S3). Ammonium bacterial abundance was observed over a wide range with high spatial heterogeneity, and much higher in surface than subsurface sediments.

The highest potential ammonium rate was observed at  $11.3 \text{ mmol N g}^{-1} \text{ h}^{-1}$  in the superficial interface sediment (site B) with the <sup>15</sup>N-tracer technique, significantly higher than that in the landward phase ( $0.8 \text{--} 1.0 \text{ mmol N g}^{-1} \text{ h}^{-1}$ , site C) and landward soils ( $0.05 \text{--} 0.14 \text{ mmol N g}^{-1} \text{ h}^{-1}$ , site D). Tukey's multiple comparisons test indicated that the ammonium oxidation rates in riparian zones have long been regarded as nitrate sinks<sup>5</sup> because of the high nitrogen input and low nitrogen output.

# 3. Applications in ecohydraulics

## □ Riparian vegetation dynamics: flow plant dynamics



# 3. Applications in ecohydraulics

## □ Riparian vegetation dynamics – flow stress

$$Y(t + \Delta t) = \begin{cases} lag \cdot b Y(t) [1 - Y(t)/K] \Delta t + Y(t) & \text{Light stress} \\ (1 - loss) \cdot Y(t) & \text{Middle stress} \\ (1 - loss) \cdot Y(t) \cdot \frac{abs[\text{sign}(\Delta r)] + \text{sign}(\Delta r)}{2} & \text{Strong stress} \end{cases}$$

Y(t + Δt) =   
 (1 - loss) · Y(t)   
 Biomass loss   
 (1 - loss) · Y(t) ·  $\frac{abs[\text{sign}(\Delta r)] + \text{sign}(\Delta r)}{2}$    
 Biomass loss & certain mortality

Ye F., et al., 2010, *Eco. Info.*, 5: 108-114

Liu R., et al., 2014, *Scientific Report*, 4: 5507

# 3. Applications in ecohydraulics

## □ Riparian vegetation dynamics – species competition

$$\Delta B_{weak} = -\Delta B_{strong} \cdot \frac{C_{strong}}{C_{weak}}$$

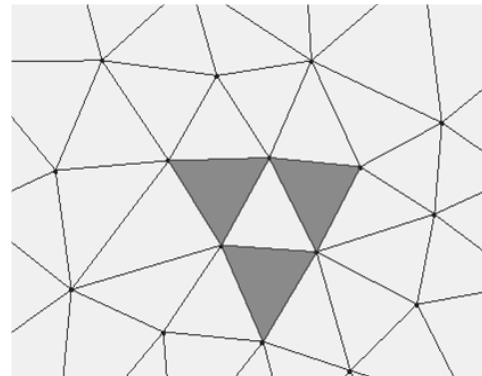
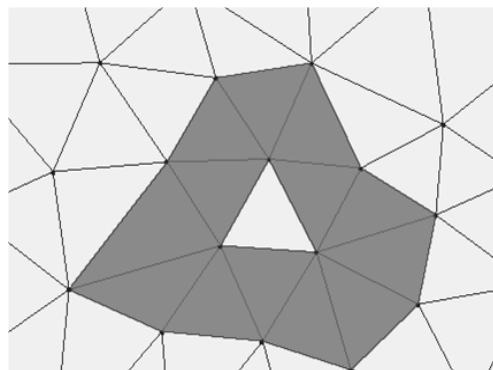
$\Delta B_{weak}$  = biomass change of weak competing species

$C_{weak}$  = source consumption rate of weak species

$\Delta B_{strong}$  = biomass change of strong competing species

$C_{strong}$  = source consumption rate of strong species

## □ Riparian vegetation dynamics – species colonization



Each species has a maximum colonization extend, depending on species physiology and field survey results

# 3. Applications in ecohydraulics

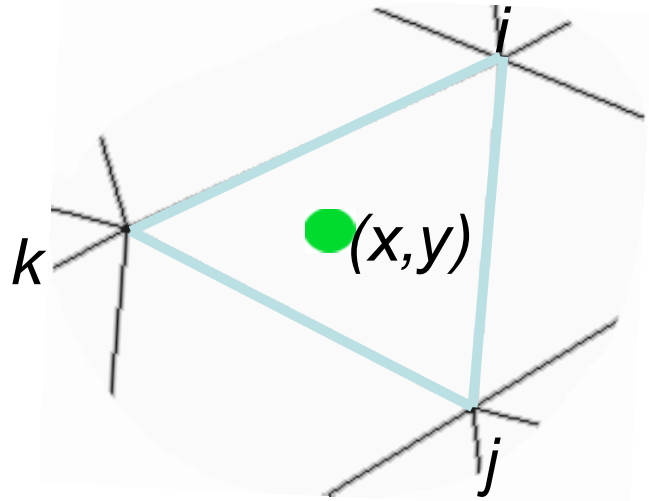
## □ Flow → Vegetation interaction

④ To each CA cell, define...

$$L_i = \frac{1}{2\Delta} (a_i + b_i x + c_i y)$$

$$L_j = \frac{1}{2\Delta} (a_j + b_j x + c_j y)$$

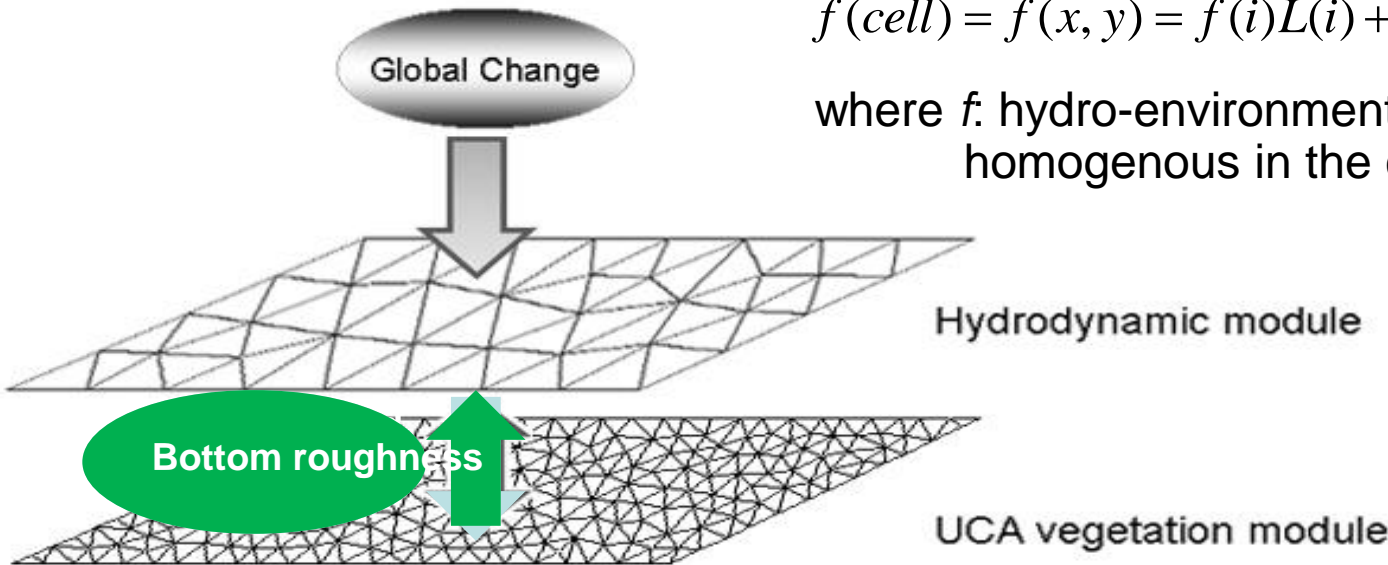
$$L_m = \frac{1}{2\Delta} (a_m + b_m x + c_m y)$$



④ To each CA cell, the hydro-environ effect

$$f(\text{cell}) = f(x, y) = f(i)L(i) + f(j)L(j) + f(k)L(k)$$

where  $f$ : hydro-environment factor, and assuming homogenous in the cell



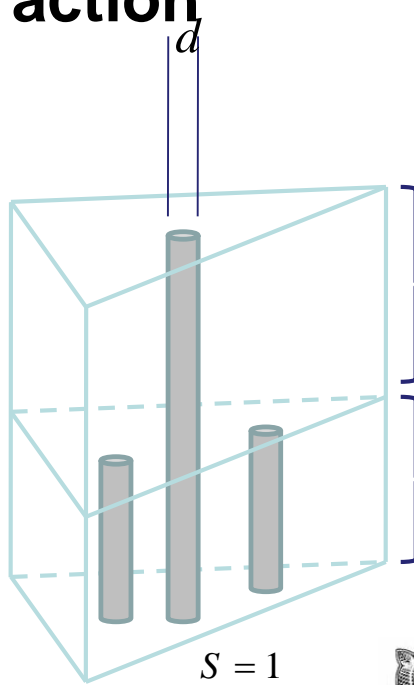
# 3. Applications in ecohydraulics

## □ Vegetation → Flow interaction

### ④ Method 1

$$C_d = \frac{g(n_b + n_{plant})^2}{R^{1/3}} \quad \lambda_{(k+1)} = 1$$

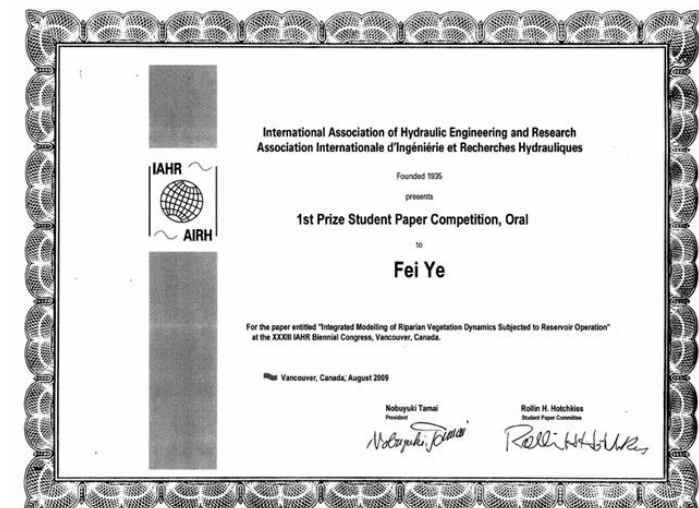
$$\lambda_{(k)} = 3$$



$$\Delta z_{(k+1)}$$

$$\Delta z_{(k)}$$

**JFK Best Student Paper,  
IAHR 2009, Vancouver**



### ④ Method 2

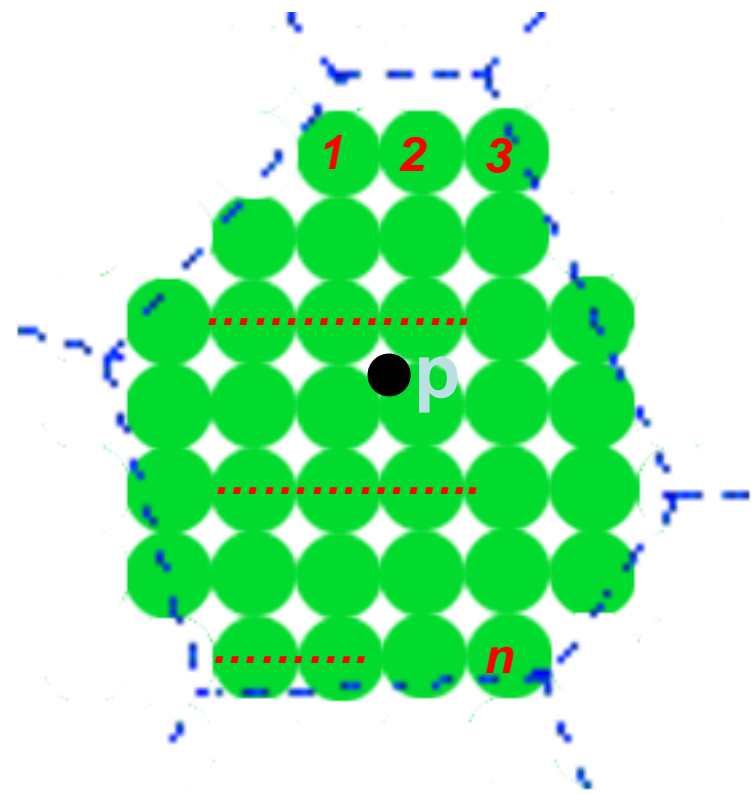
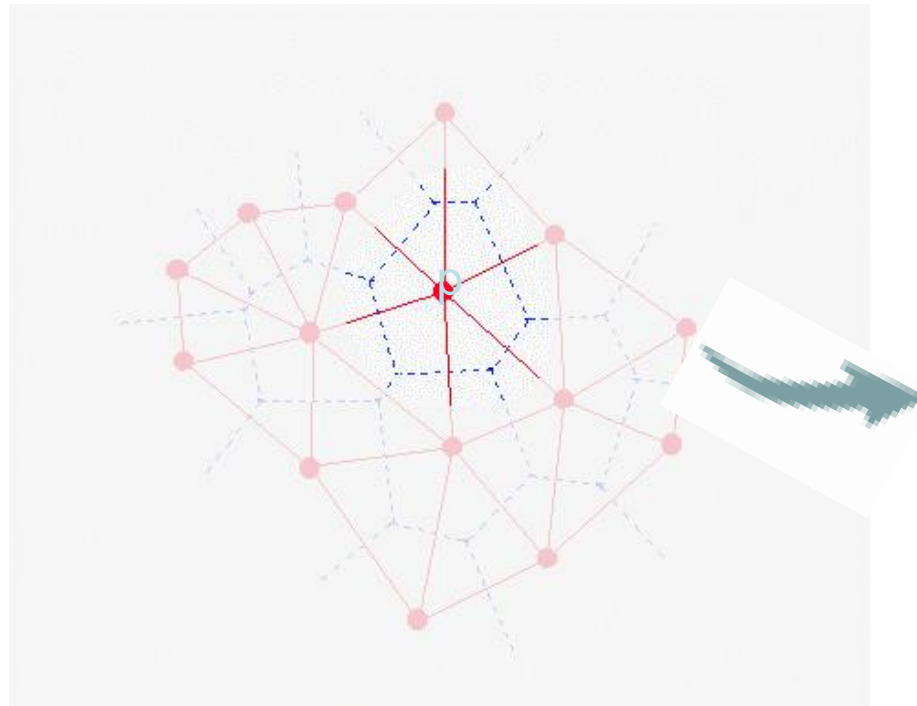
$$F_D = \frac{1}{2} C'_d \lambda \rho U^2$$

### ④ Method 3

$$F_D = \frac{1}{2} C'_d \rho U^2$$

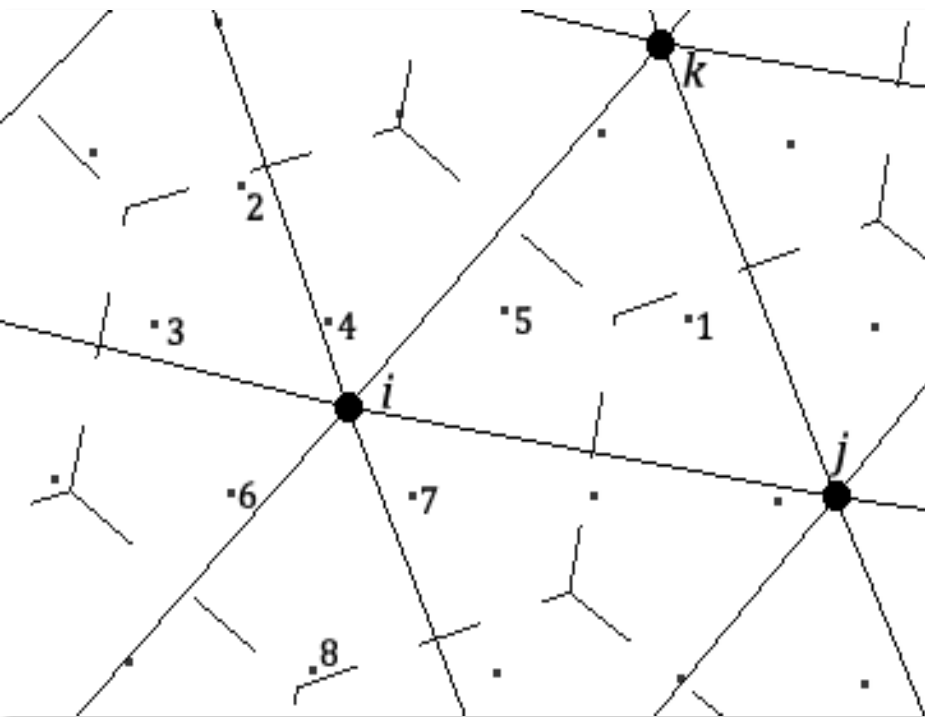
# 3. Applications in ecohydraulics

## □ Vegetation → Flow interaction



$$Rough_{node}(P) = \sum_{i=1}^n rough_{cell}(i) \frac{area(i)}{\sum_{i=1}^n area(i)}$$

# 3. Applications in ecohydraulics



Flow → Plant

$$f_{plant}(1) = f_{plant}(x_c, y_c) = \\ f_{hydro}(i)L_i + f_{hydro}(j)L_j + f_{hydro}(k)L_k$$

$$\begin{cases} L_i(x, y) = \frac{(x_j y_k - x_k y_j) + (y_j - y_k)x + (x_k - x_j)y}{2\Delta_{ijk}} \\ L_j(x, y) = \frac{(x_k y_i - x_i y_k) + (y_k - y_i)x + (x_i - x_k)y}{2\Delta_{ijk}} \\ L_k(x, y) = \frac{(x_i y_j - x_j y_i) + (y_i - y_j)x + (x_j - x_i)y}{2\Delta_{ijk}} \end{cases}$$

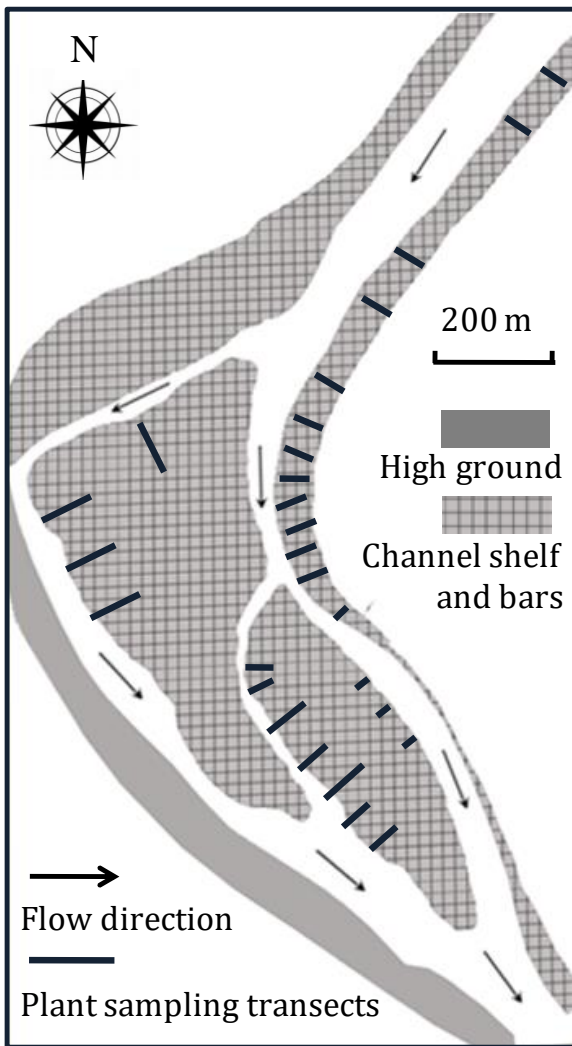
Plant → Flow

$$f_{hydro}(i) = \sum_{n=2}^8 f_{plant}(n)w(n)$$

$$w(n) = \Delta_n / \Delta_{ijk}$$

# 3. Applications in ecohydraulics

## □ Riparian vegetation dynamics – study area



### Location

Middle reach of Lijiang River: 25° 06' N, 110° 25' E

### Flow condition

2009.01~2010.12 : 20~3720m<sup>3</sup>

### Vegetation survey

Several transects were surveyed, each transect have 5 squares in **S** shape:



*Rumex Maritimus*:  
Near water, averagely  
3/m<sup>2</sup>, relatively tall.

*Leonurus Heterophyllus*:  
near the bank, away from  
the water. averagely 1/m<sup>2</sup>

*Polygonum Hydropiper*:  
In between, averagely  
32/m<sup>2</sup>~35/m<sup>2</sup>

# 3. Applications in ecohydraulics

## □ Riparian vegetation dynamics – modeled species

*R. Maritimus*



*Rumex maritimus*

*P. Hydropiper*



*Polygonum  
hydropiper*

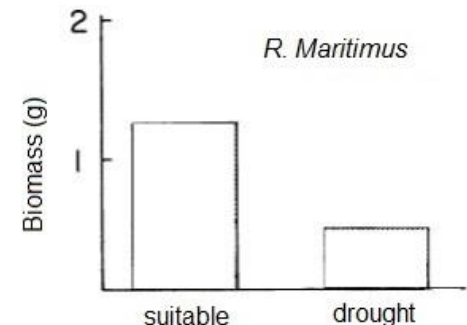
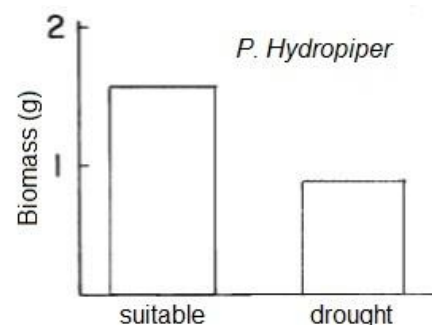
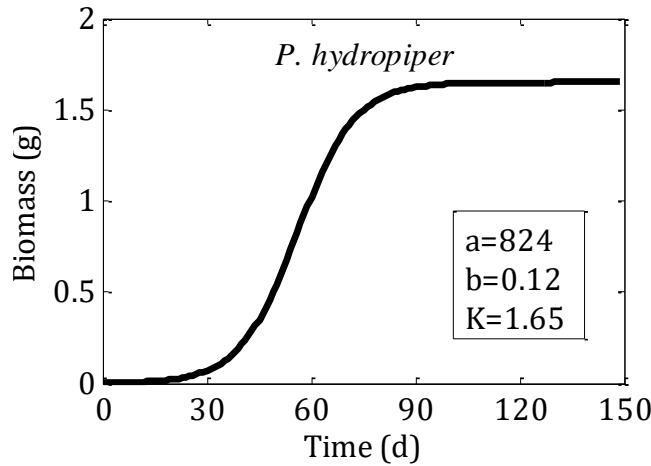
*L. Heterophyllus*



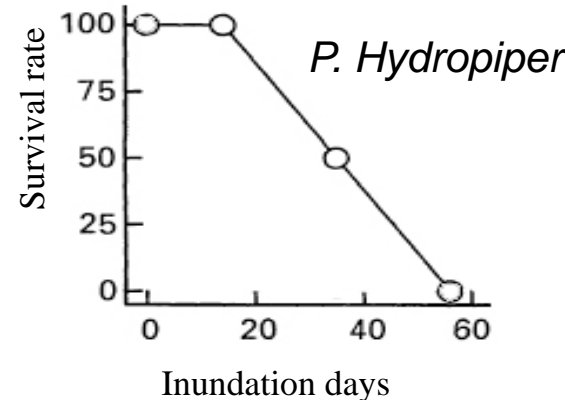
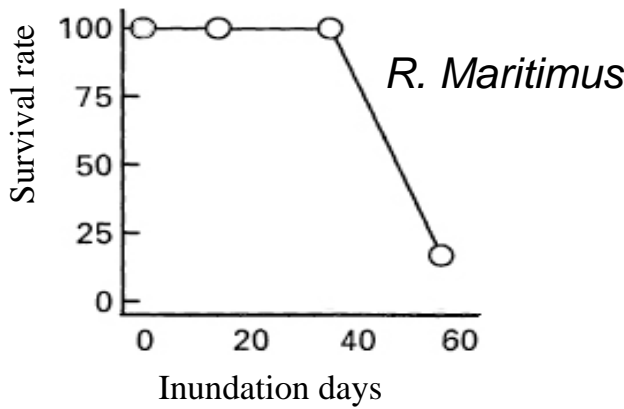
*Leonurus heterophyllus*

# 3. Applications in ecohydraulics

## □ Riparian vegetation dynamics – flow stress

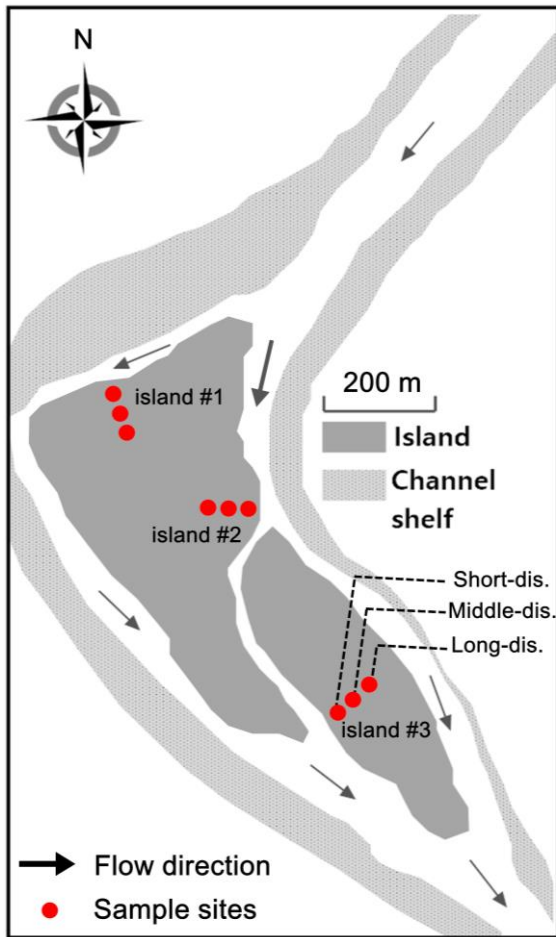


Transform to **discrete form**:  $Y(t + \Delta t) = bY(t)[1 - Y(t)/K]\Delta t + Y(t)$



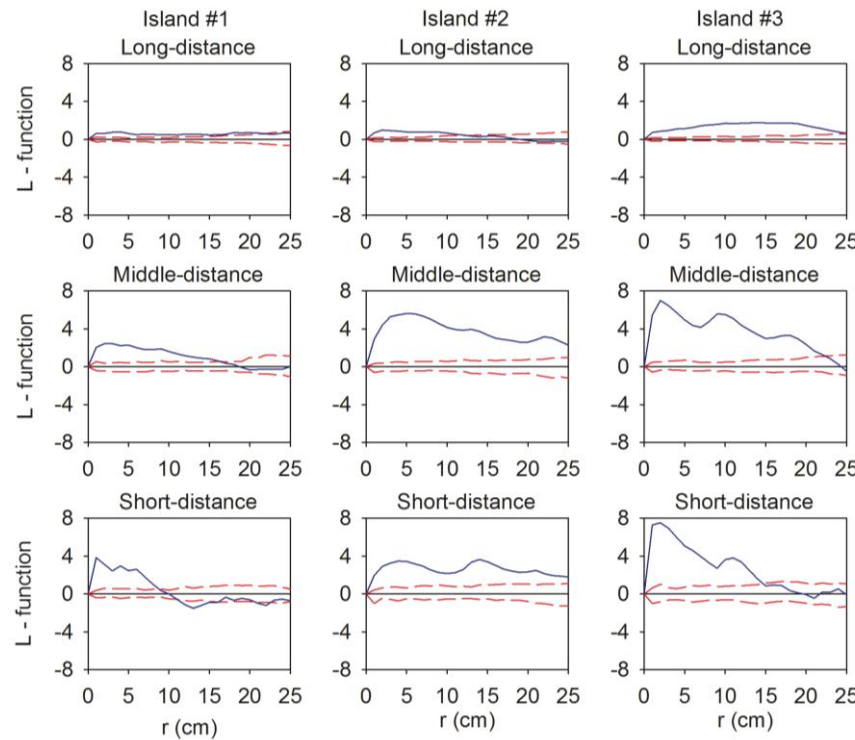
# 3. Applications in ecohydraulics

## □ Riparian vegetation dynamics – the scales



### Ⓐ Ripley L function

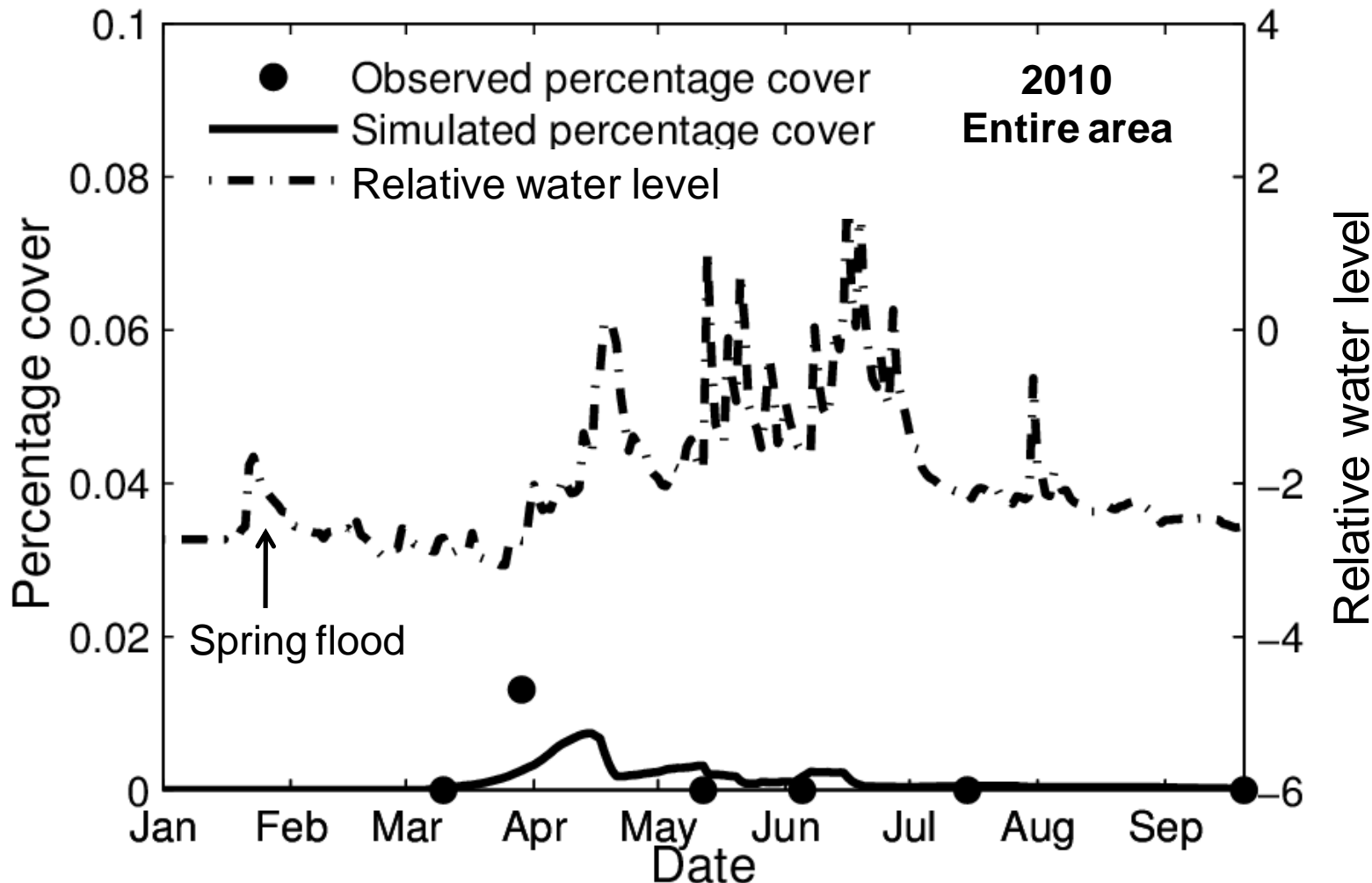
$$L(r) = \sqrt{\frac{K(r)}{\pi}} - r \quad K(r) = \frac{A}{n^2} \sum_{i=1}^n \sum_{j=1}^n \frac{I_r(d_{ij})}{w_{ij}}$$



⌚ $x = r/2$ , ⌚ $t = 9$  hours

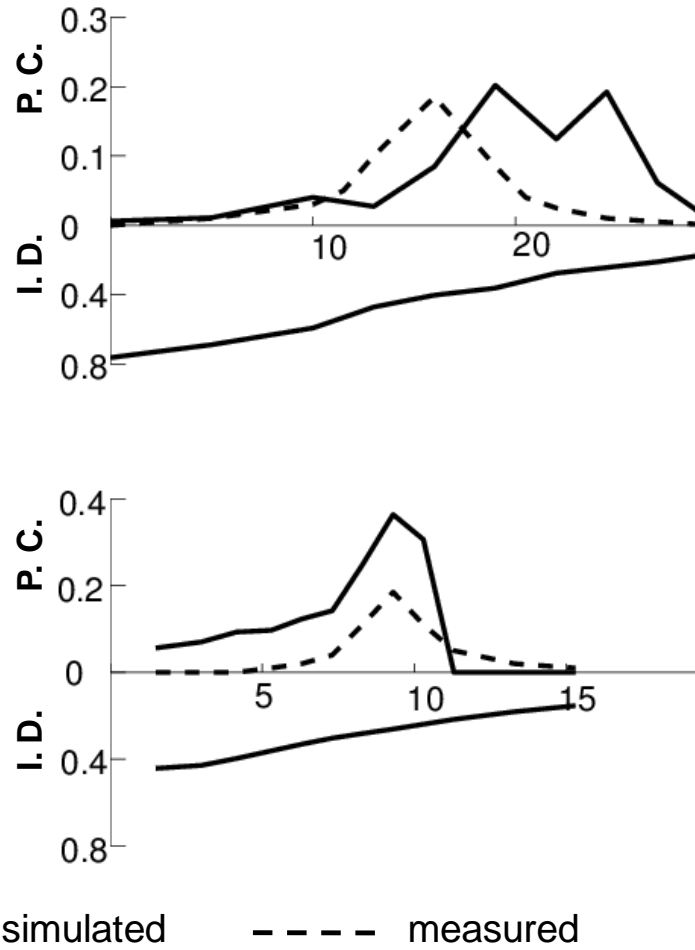
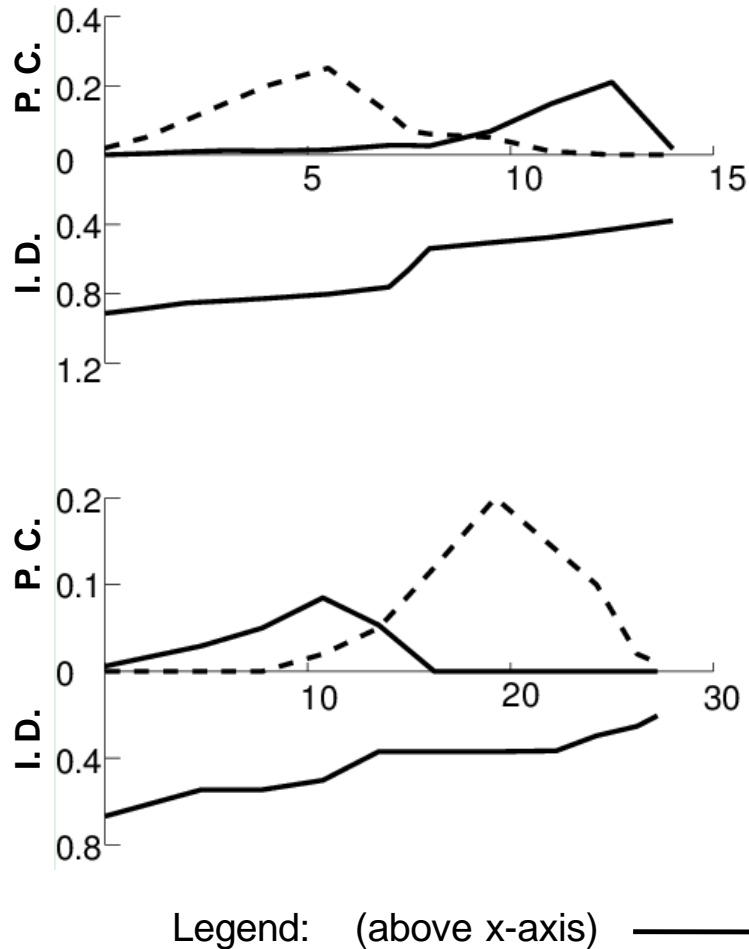
### 3. Applications in ecohydraulics

#### □ *P. hydropiper* dynamics in 2010 – model validation



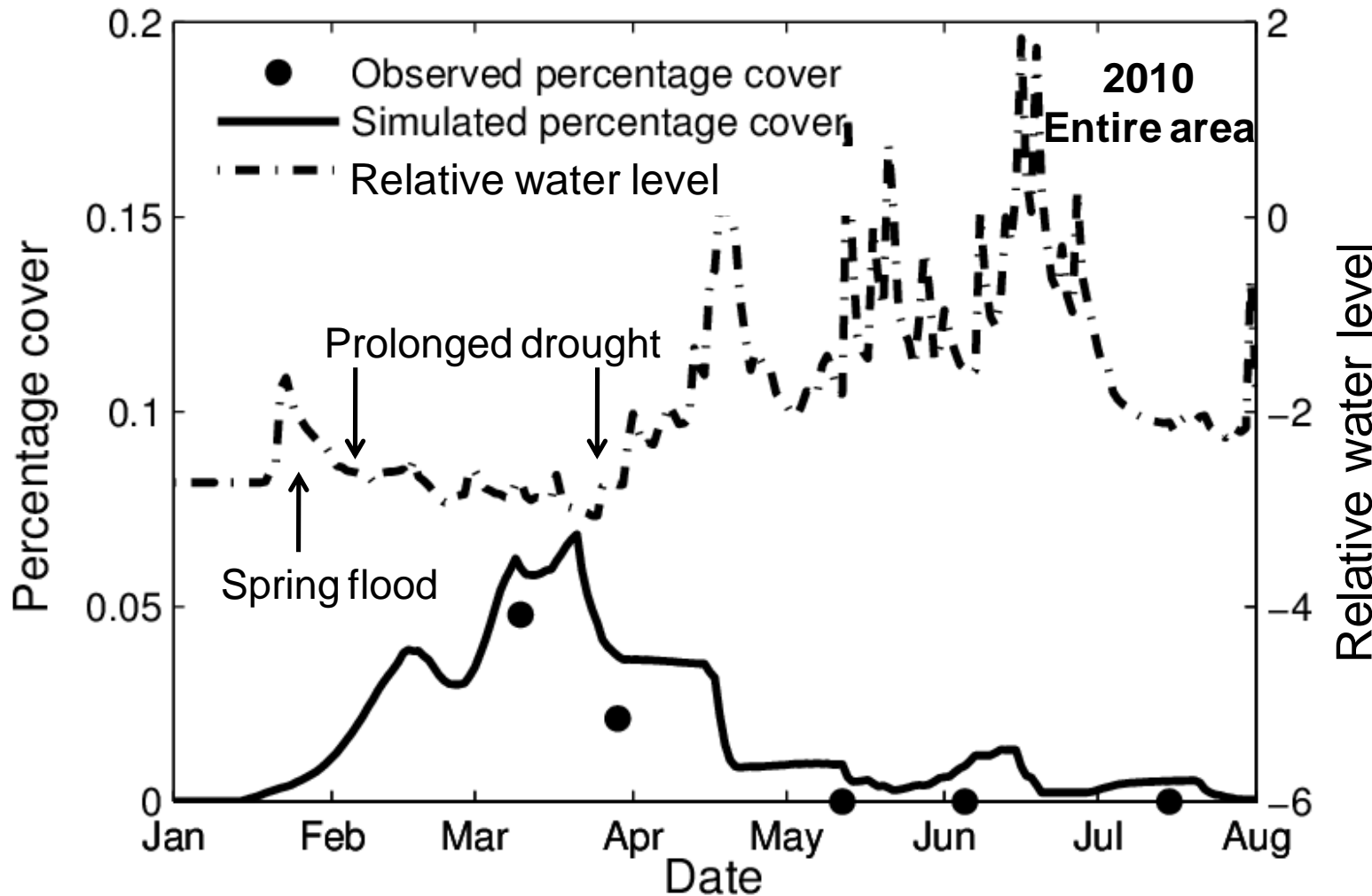
# 3. Applications in ecohydraulics

## □ *P. hydropiper* transect in 2010 – model validation



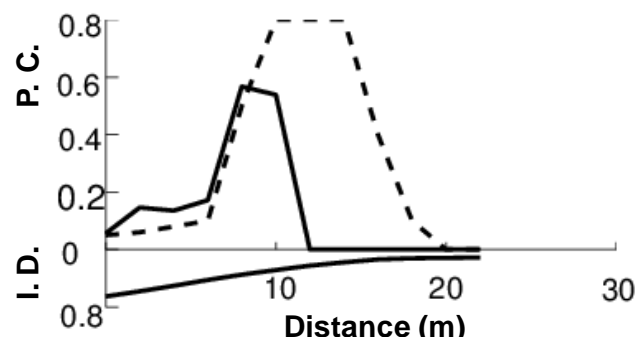
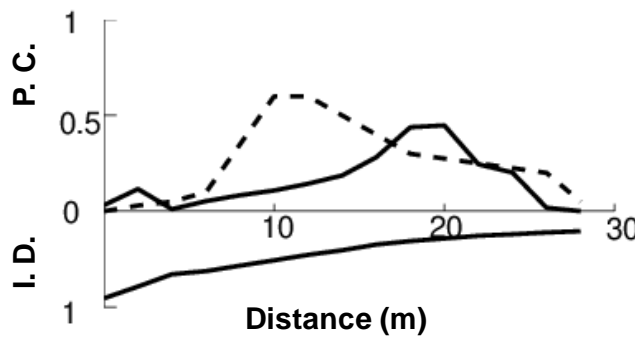
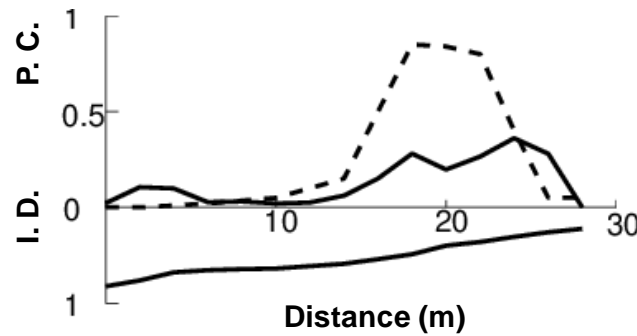
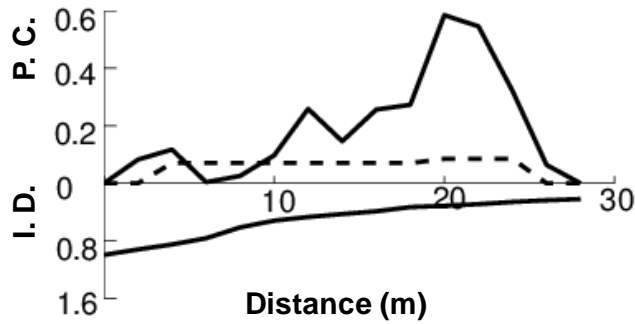
### 3. Applications in ecohydraulics

#### □ *R. maritimus* dynamics in 2010 – model validation



# 3. Applications in ecohydraulics

## □ *R. maritimus* transect in 2010 – model validation



Legend: (above x-axis) — simulated    - - - measured

# 3. Applications in ecohydraulics

## □ Riparian vegetation dynamics – model comparison

$$\begin{aligned}\log(Y) = & -49.3294 + 62.4774 \cdot i - 43.9644 \cdot i^2 \\ & + 74.3 \cdot aw - 58.623 \cdot aw^2 \\ & + 11.3704 \cdot mw - 23.2815 \cdot mw^2 \\ & + 7.6828 \cdot ad\end{aligned}$$

$Y$ : coverage of vegetation (*P. hydropiper*) by the end of growth period;

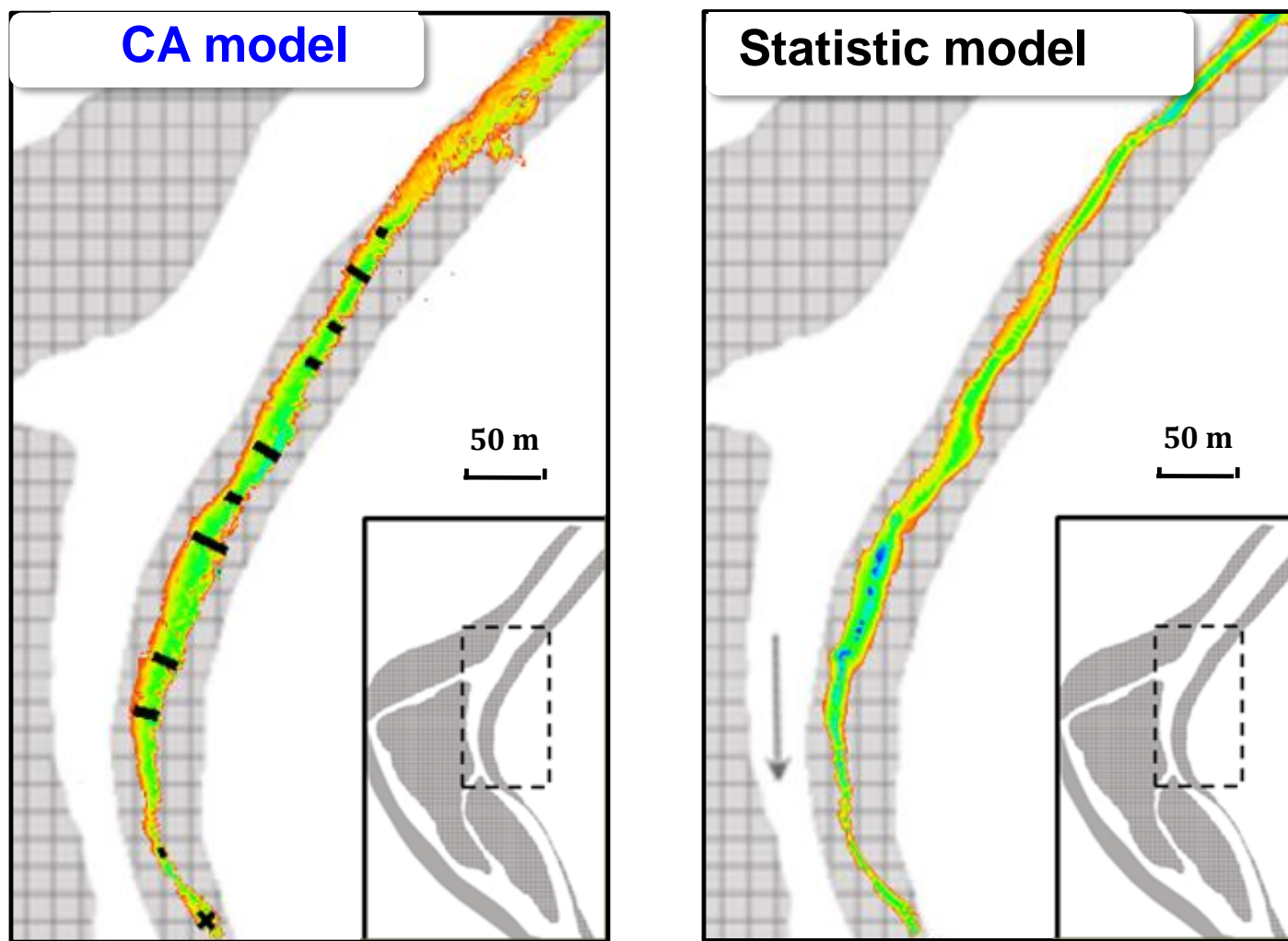
$i$ : ratio of inundation time;

$mw$ : maximum inundation time;

$aw$ : averaged inundation depth;

$ad$ : ground water depth.

# 3. Applications in ecohydraulics



Legend:



Channel shelf and bars

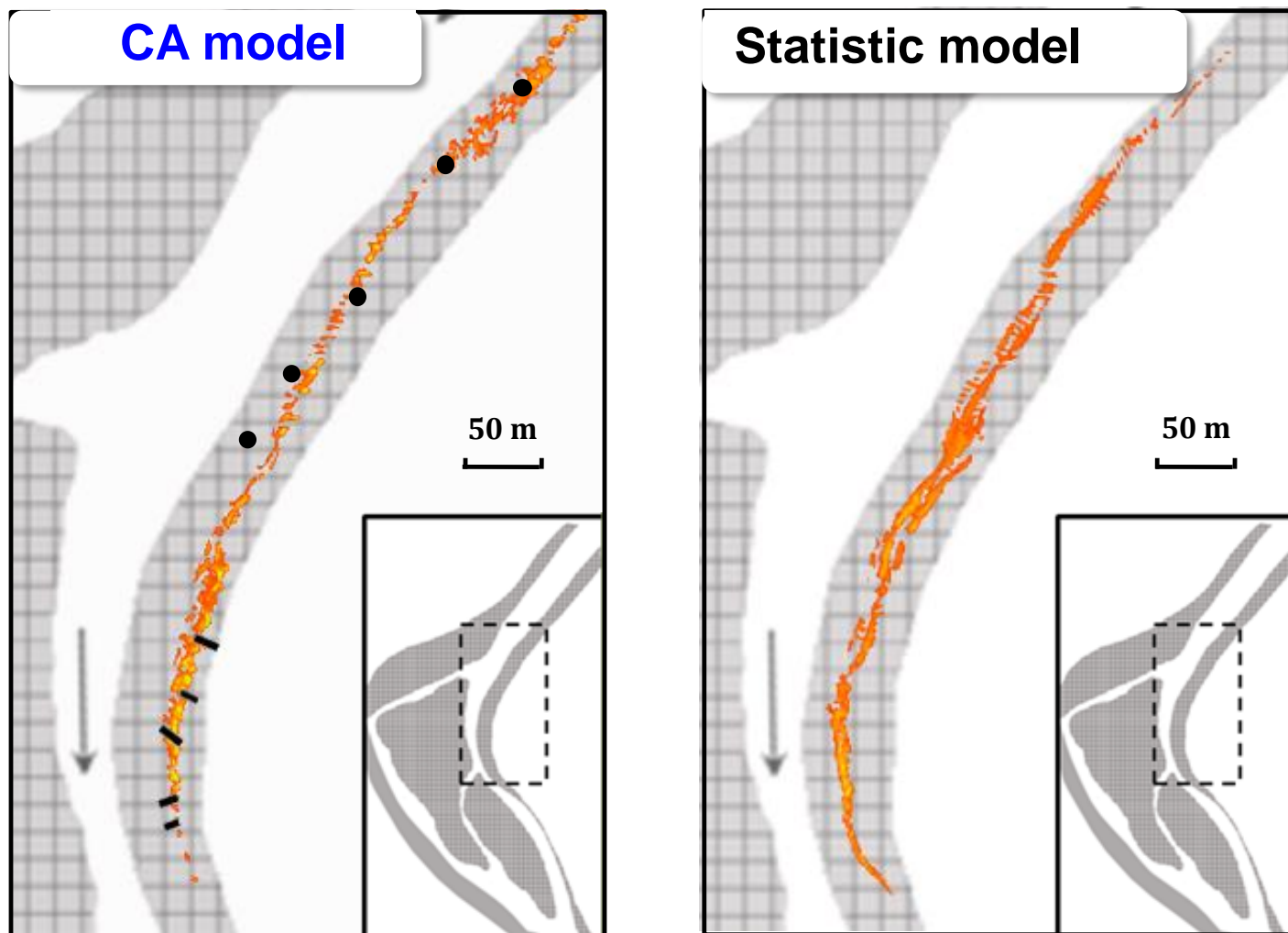


Flow direction

• Sampled transects: Location and length of plant belt • Quadrats with <5% cover

• Simulated percent cover: 0% 100%

# 3. Applications in ecohydraulics



Legend:



Channel shelf and bars



Flow direction

• Sampled transects: — Location and length of plant belt • Quadrats with <5% cover

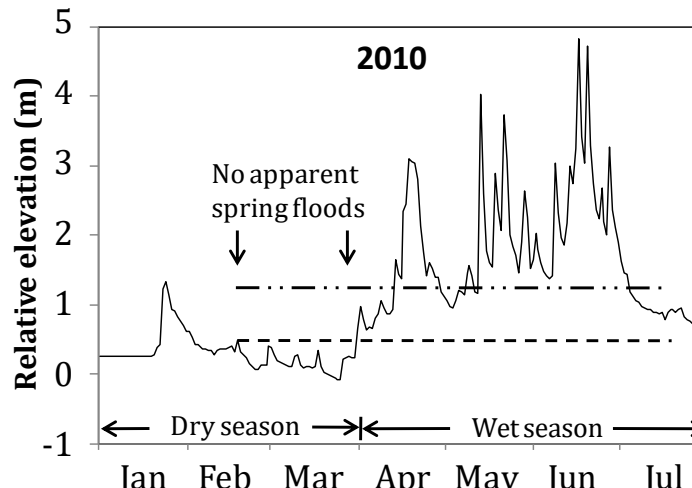
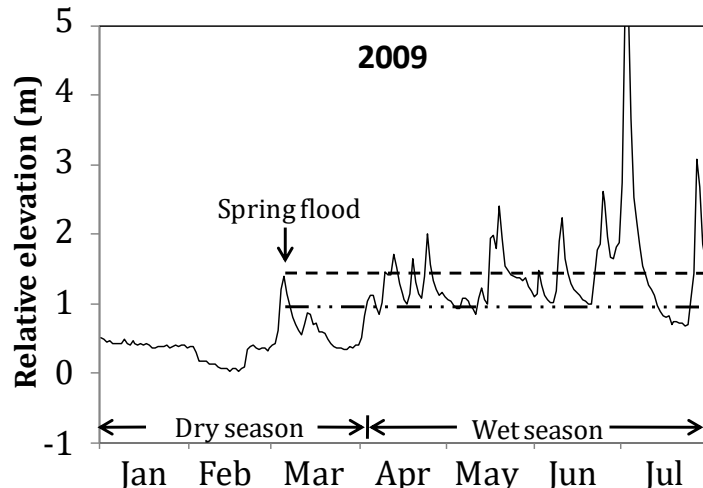
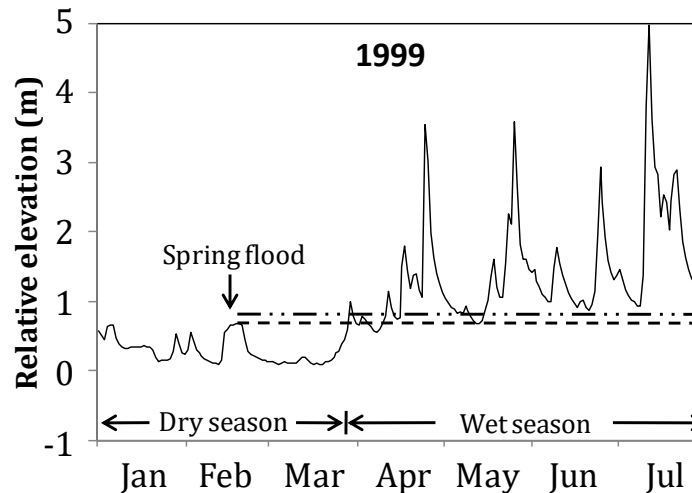
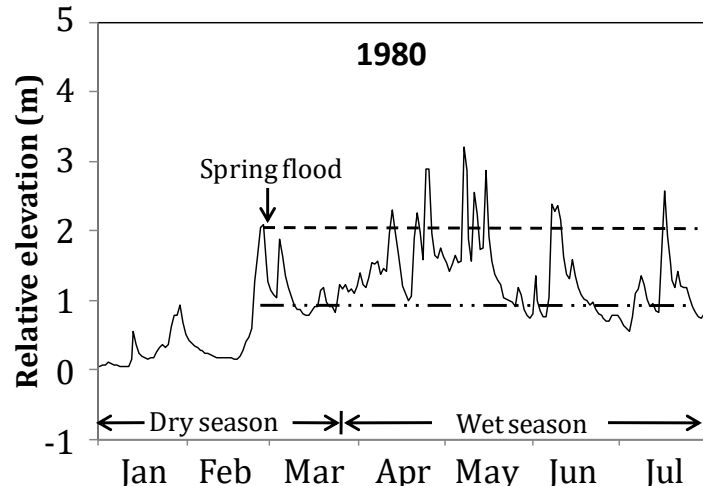
• Simulated percent cover: 0%



100%

# 3. Applications in ecohydraulics

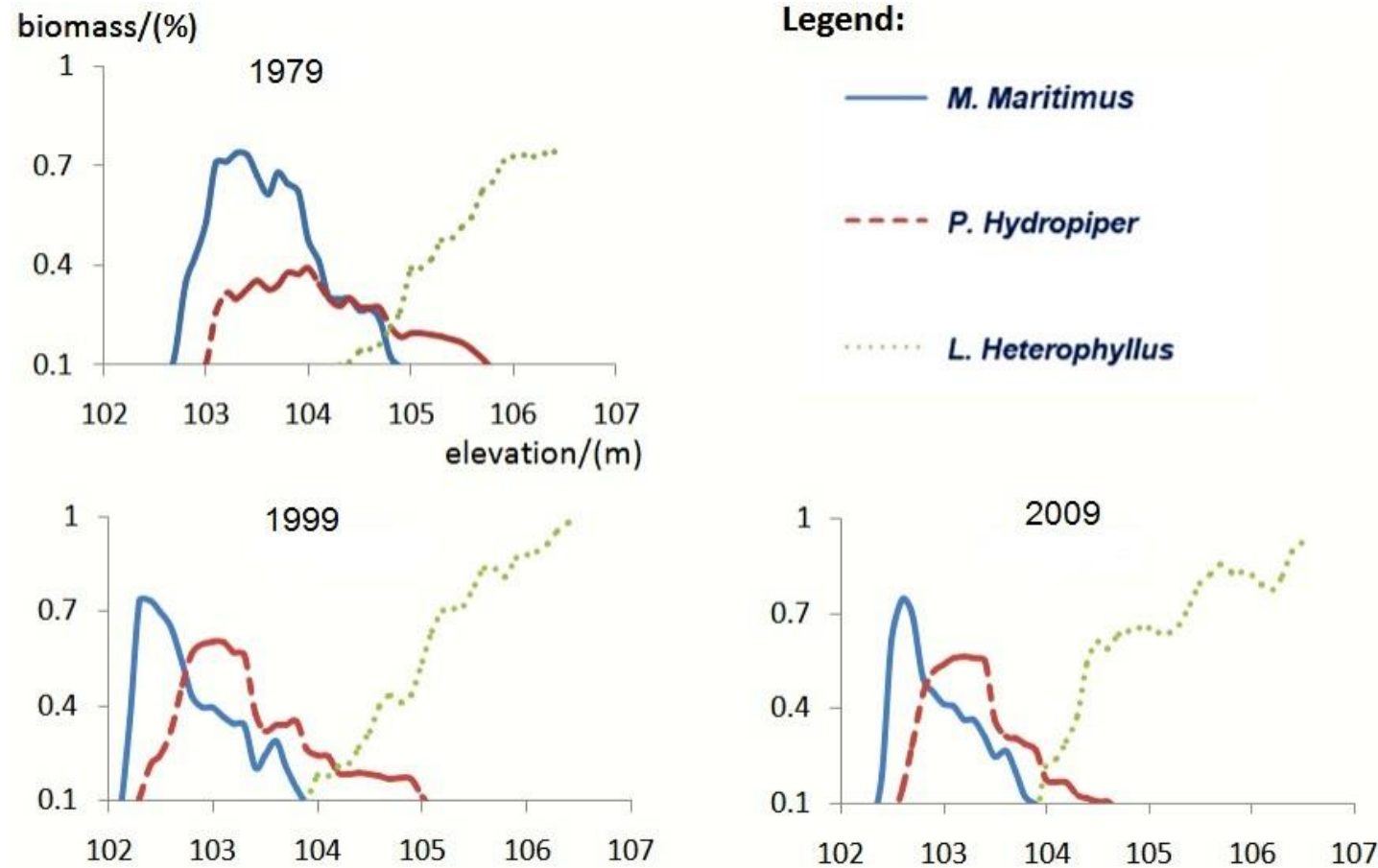
## □ Riparian vegetation dynamics – vegetation succession



Legend: - - - upper bound constrained by spring floods  
— · · · lower bound constrained by wet season floods

# 3. Applications in ecohydraulics

## □ Riparian vegetation dynamics – vegetation succession

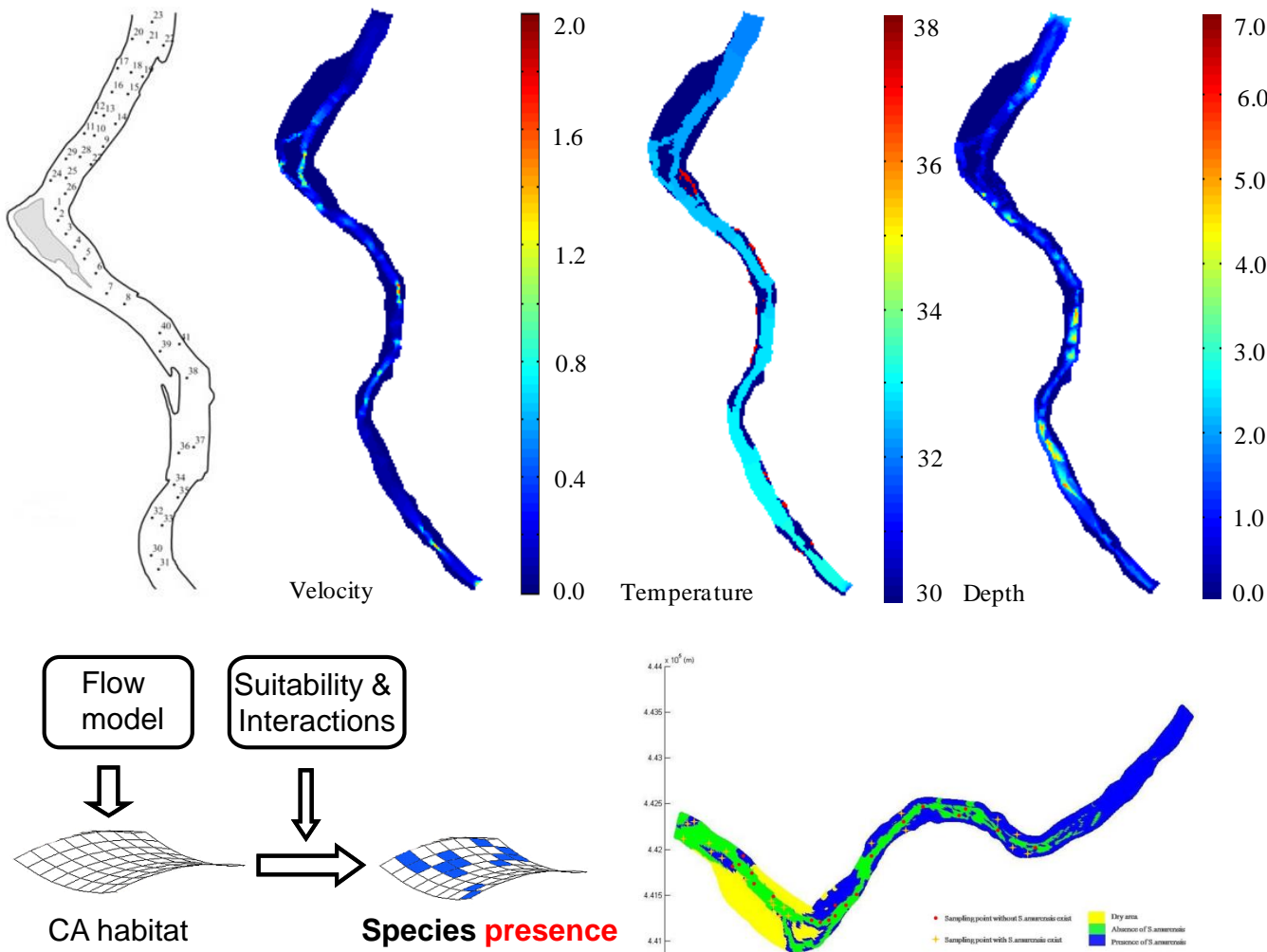
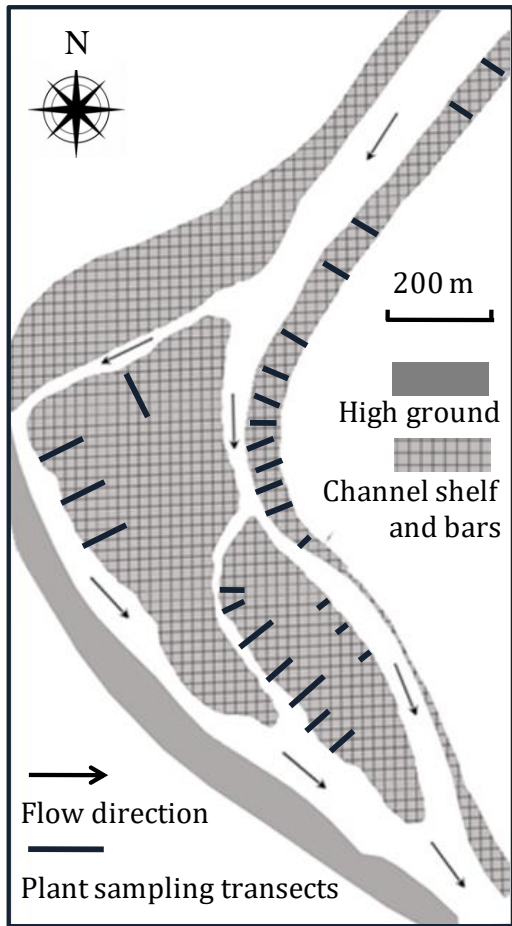


Ye F., et al., 2010, *Eco Inf*, 5: 108-114;

Liu R., et al., 2014, *Scientific Report*, 4: 5507

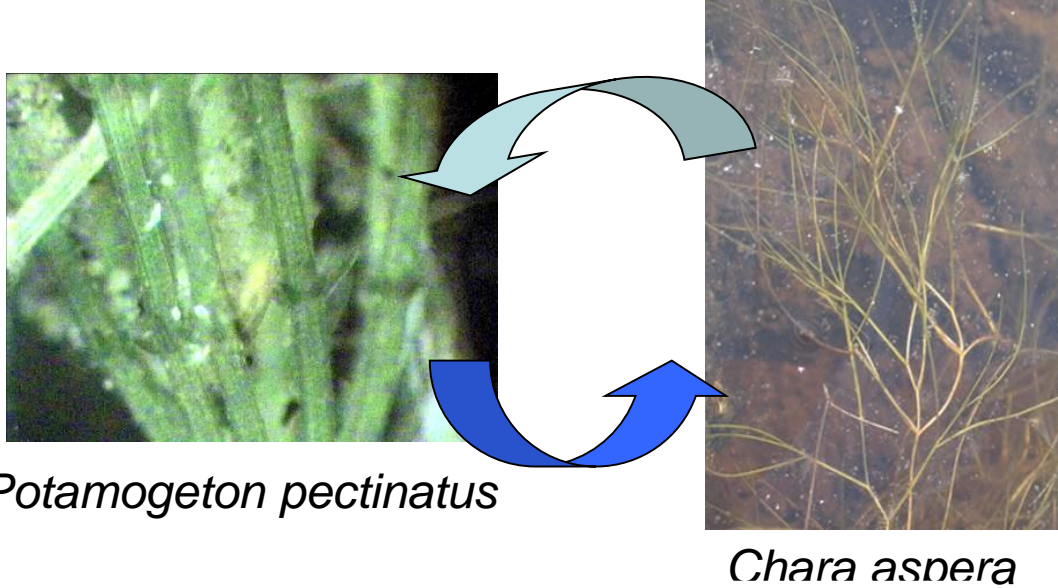
# 3. Applications in ecohydraulics

## □ River macroinvertebrates inhabitant: flow → local movement



# 3. Applications in ecohydraulics

## □ Macrophytes succession: vertical mixing → local competition



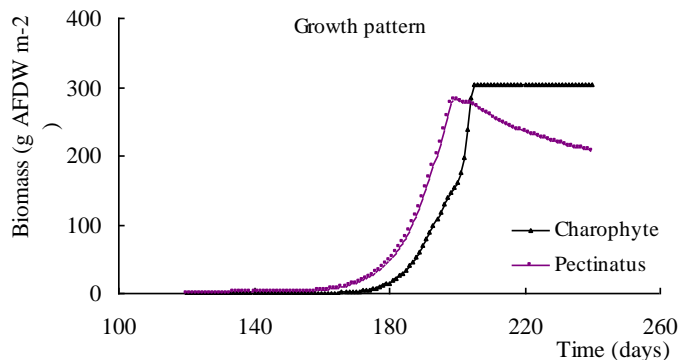
Before 1968, various species

Eutrophication

1970~1989, algae and *Potamogeton pectinatus*

Restoration

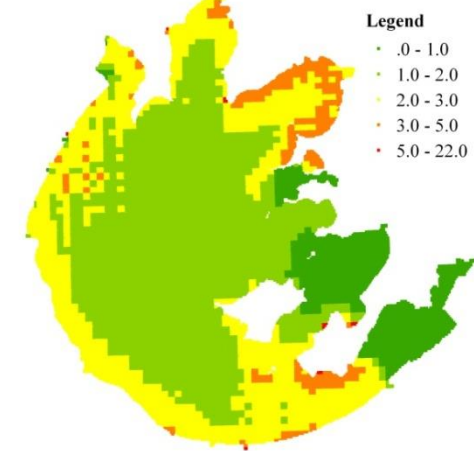
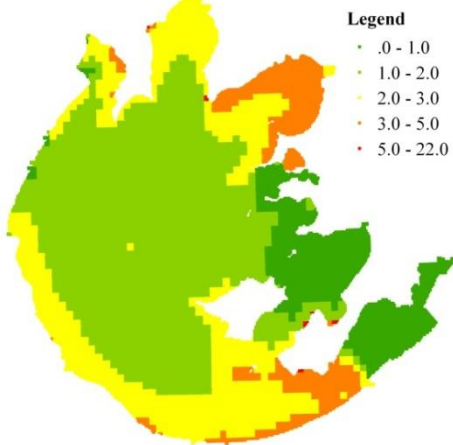
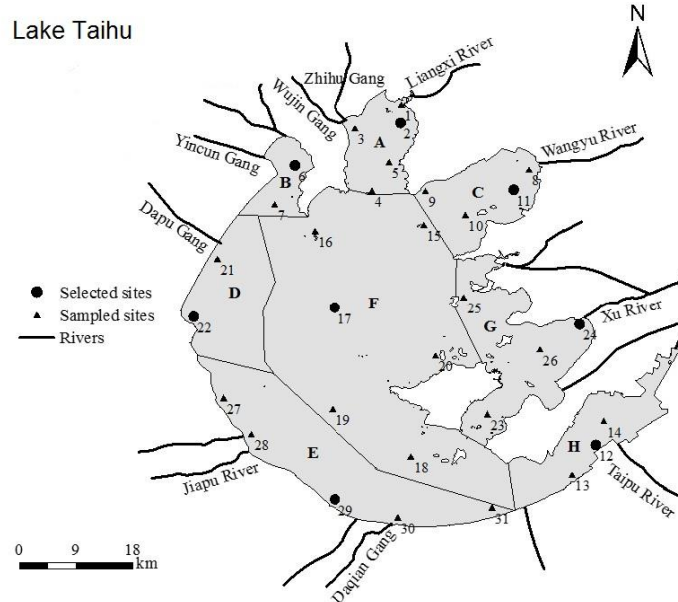
1990~, *Chara aspera* back and dominant



Chen and Mynett., 2003, *Eco Mod*,  
147: 253-262 (Citations: 53)

# 3. Applications in ecohydraulics

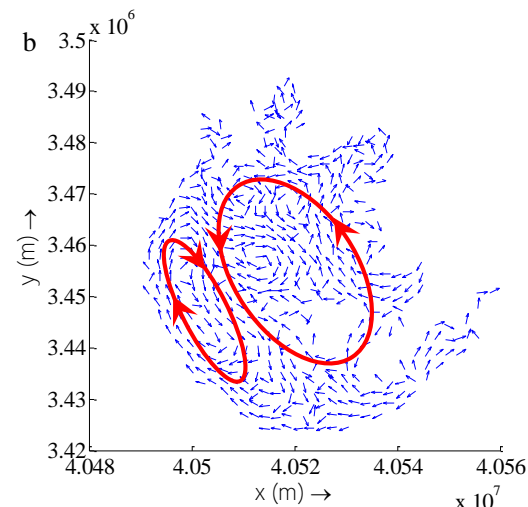
□ Lake algae bloom: flow + wind drifting → algae patchiness



$$R_i^{t+2} = (7.66 + NO_{3i}^t + 0.0441 * WT_i^t - 0.14 * PO_{4i}^t) / (1.2 + (NO_{3i}^t)^2)$$

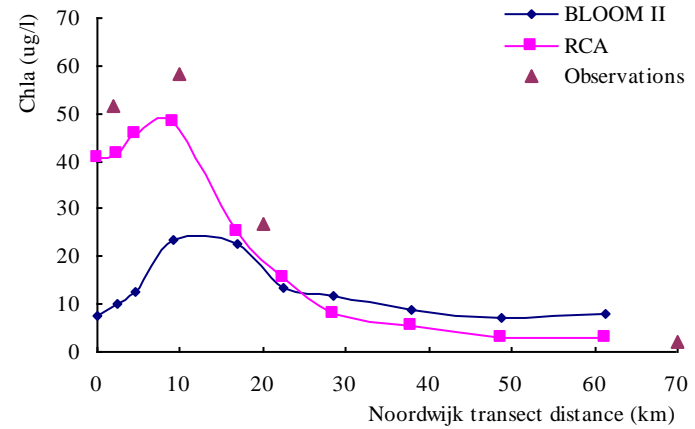
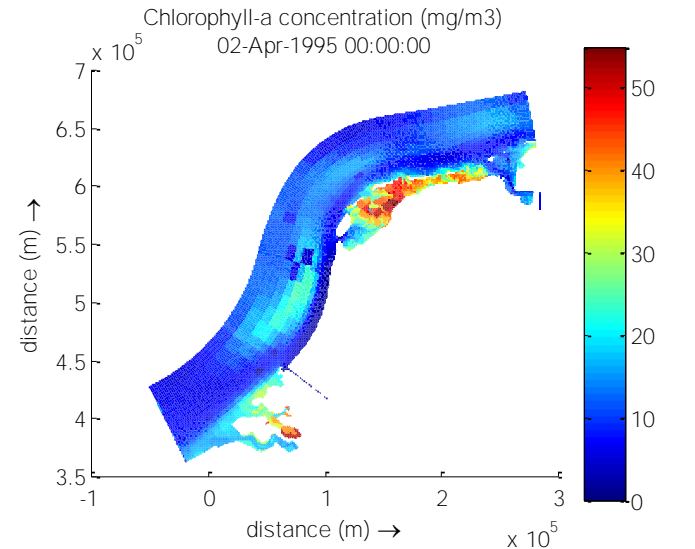
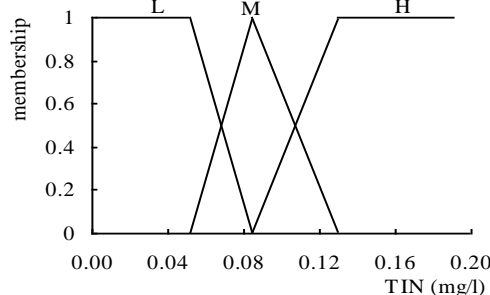
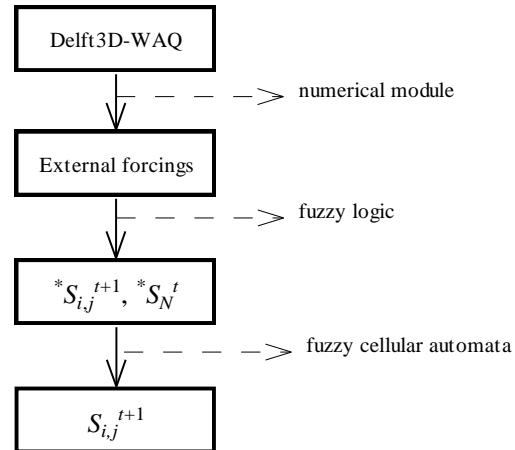
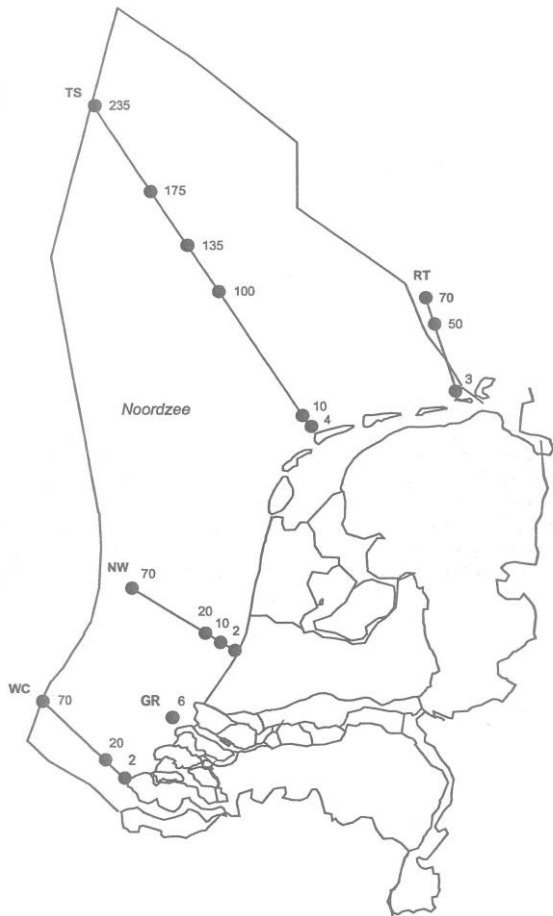
$$C_i^{t+2} = R_i^{t+2} + C_i^t \quad C_i^{t+2} = a_i C_i^{t+2} + \sum a_j C_j^{t+2}$$

❖  $\Delta t$ : 12 hours in algae model; cell size  $\Delta x$ : drifting speed  $\times \Delta t$



# 3. Applications in ecohydraulics

## □ Coastal algal bloom: current → algae patchiness

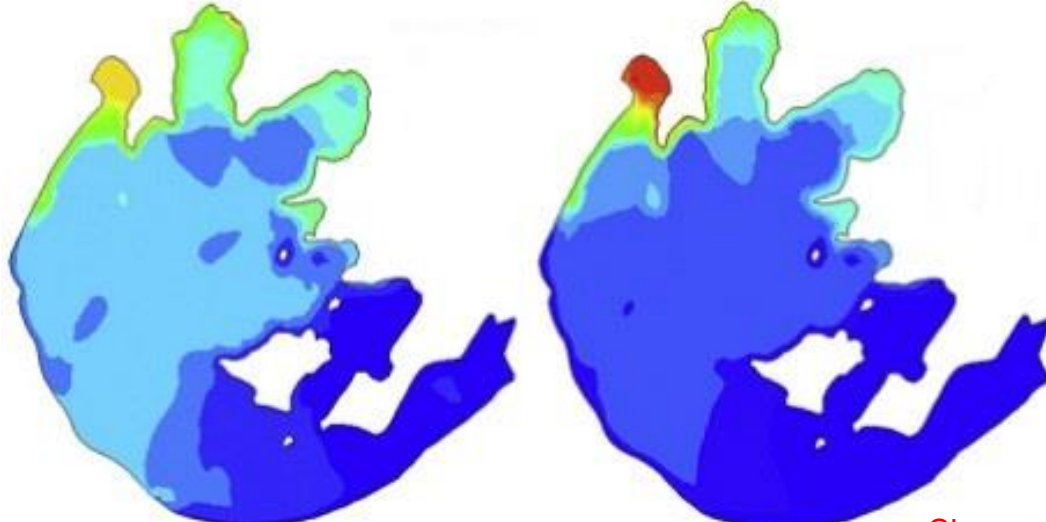


# 3. Applications in ecohydraulics

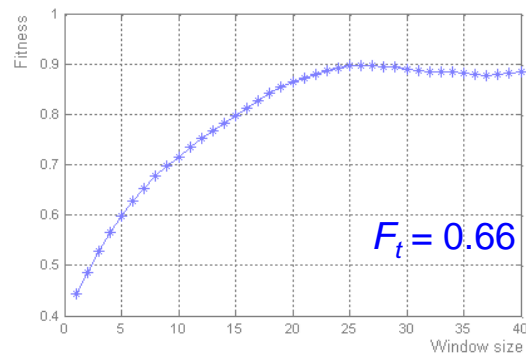
## □ Spatially-explicit evaluation of CA model

model	1x1 window	observation
1 1 1 1 2 2 2 2 3 3 3 3	F = 1	1 1 2 2 2 2 2 2 3 3
1 1 1 2 2 2 2 3 3 3 3 3	2x2 window	1 1 1 1 2 3 3 3 3 3
1 1 2 2 2 3 3 3 3 3 3 3	F = 1 - 4/8 = .50	1 1 1 2 3 3 3 3 3 3
3 3 2 2 3 3 3 3 3 3 3 3		3 1 2 2 3 3 3 4 4 4
1 3 3 3 3 3 3 3 3 3 3 3		3 3 3 3 3 3 3 3 3 3
1 1 1 3 3 3 3 3 3 3 3 3		1 1 1 3 3 3 3 3 3 3
2 2 2 2 2 2 2 2 3 3 3	3x3 window	1 1 2 2 2 2 2 2 3 3
3 3 3 3 3 3 3 3 3 3 3 3	F = 1 - 6/18 = .6667	1 2 2 3 3 2 2 3 3 3
3 3 3 3 3 2 2 3 3 3 3 3		3 3 3 3 2 2 2 3 3 3
3 3 3 3 3 2 2 2 2 3 3 3		3 3 3 3 2 2 2 2 3 3

R. Costanza, *Ecol. Mod.*, 1989



$$F_w = \frac{\sum_{i=1}^{t_w} |a_{1i} - a_{2i}|}{2w^2}$$
$$F_t = \frac{\sum_{w=1}^n F_w e^{-k(w-1)}}{\sum_{w=1}^n e^{-k(w-1)}}$$



# Final remarks

- (1) Through hierarchical scale coupling, the fluid dynamics is linked to aquatic eco-dynamics
- (2) The adoption of cellular automata offers a novel approach to describe aquatic eco-dynamics featured by spatial heterogeneity, local interactions and discrete processes
- (3) The developed ecohydraulic models provide a broad range of applications with promising potential.

# The persons & the path.....



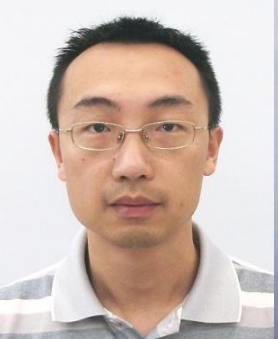
Prof. Arthur Mynett



Dr. Tony Minns



Ruonan Li



Fei Ye



Koen Blanckaert



Yुqing Lin



Rui Han



Xiaoqing Zhang

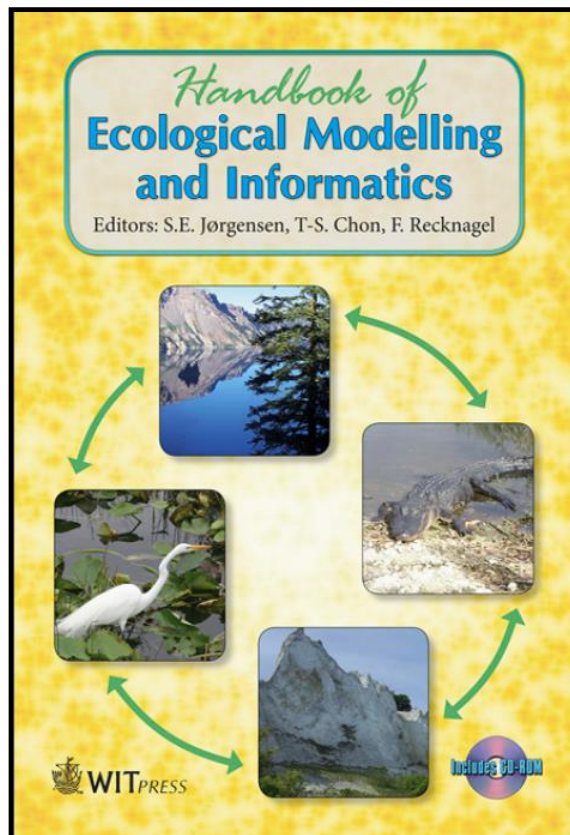
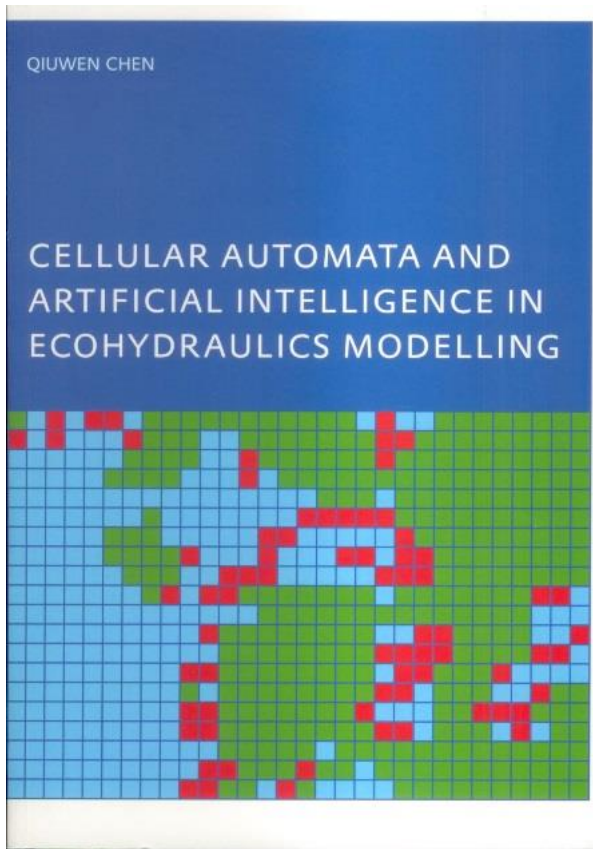


Qingrui Yang

# For more information.....

● [qwchen@nhri.cn](mailto:qwchen@nhri.cn)

● 34 Hujuguan, NHRI, China

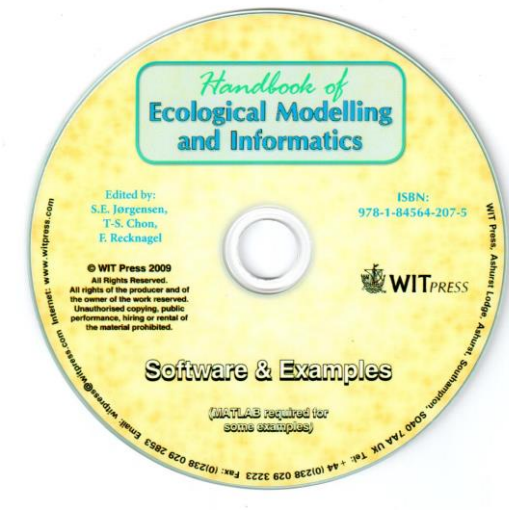


## CHAPTER 16

### Cellular automata

Q. Chen

State Key Laboratory of Urban and Regional Ecology, Research Center for Eco-Environmental Sciences, Chinese Academy of Sciences, Beijing China.



A scenic landscape featuring a calm lake in the foreground, rocky hillsides covered in green vegetation, and a clear blue sky. A herd of white sheep is grazing on the left bank of the lake.

Thank You !

i hoy kunaht